Stony Brook University

Interplay between *Francisella tularensis* and Hepatocytes

A Dissertation Presented

by

Huaixin Zheng

to

The Graduate School

in Partial Fulfillment of the

Requirements

for the Degree of

Doctor of Philosophy

in

Molecular and Cellular Biology

Stony Brook University

December 2010

Stony Brook University

The Graduate School

Huaixin Zheng

We, the dissertation committee for the above candidate for the
Doctor of Philosophy degree,
hereby recommend acceptance of this dissertation.

Martha B. Furie, Ph.D., Dissertation Advisor
Professor, Department of Pathology

David G. Thanassi, Ph.D., Chair of the Committee
Professor, Department of Molecular Genetics and Microbiology

Jorge L. Benach, Ph.D.
Professor, Department of Molecular Genetics and Microbiology

Howard B. Fleit, Ph.D.
Associate Professor, Department of Pathology

Richard R. Kew, Ph.D.
Associate Professor, Department of Pathology

James B. Bliska, Ph.D.
Professor, Department of Molecular Genetics and Microbiology

This dissertation is accepted by the Graduate School.

Lawrence Martin
Dean of the Graduate School

Abstract of the Dissertation

Interplay between *Francisella tularensis* and Hepatocytes

by

Huaixin Zheng

Doctor of Philosophy

in

Molecular and Cellular Biology

Stony Brook University

2010

Francisella tularensis is the bacterial cause of tularemia and has been designated as a potential bioweapon due to its high infectivity and virulence. *F. tularensis* infects the liver of its mammalian hosts and replicates in hepatocytes, the major cells of the liver, both *in vivo* and *in vitro*. However, the factors that govern adaptation of *F. tularensis* to the intra-hepatocytic niche have not been identified. Using cDNA microarrays, we determined the transcriptional profile of the live vaccine strain (LVS) of *F. tularensis* growing in the FL83B murine hepatocytic cell line. Expression of 53 genes was up-regulated more than 2-fold compared with organisms cultured in broth. The *fslC* gene of the *fsl* operon was the most highly up-regulated (about 13-fold). In-frame deletion of *fslC* eliminated the ability of the LVS to produce siderophores, which are involved in uptake of ferric iron, and inhibited growth of the bacterium in iron-restricted media.

In-frame deletion of *feoB*, which encodes a putative bacterial ferrous iron transporter, also retarded replication of the LVS in iron-restricted media. Growth of the Δ*fslC* and Δ*feoB* mutants was the same as the wild-type LVS in human monocyte-derived macrophages. In FL83B hepatocytic cells, replication of the Δ*feoB* strain was diminished, whereas growth of the Δ*fslC* mutant was normal. However, growth of both mutants was inhibited in hepatocytes depleted of intracellular iron. Furthermore, the virulence of both mutant strains was attenuated in mice infected intranasally. FeoB thus represents a previously unidentified pathway for uptake of ferrous iron in *F. tularensis*, and our results show that both FeoB and FslC contribute to virulence of the bacterium.

Microarray analysis also was performed to determine how hepatocytes respond to infection with the *F. tularensis* LVS. Murine AML12 hepatocytes infected in vitro up-regulated expression of genes encoding proinflammatory cytokines, chemokines, colony-stimulating factors (CSF), and an adhesion molecule that binds immune cells. Enhanced production of CSF-3 and the chemokines CXCL2 and CCL20 was verified at the protein level by immunoassay. These results suggest that hepatocytes may play an important role in host defense against *F. tularensis* by recruiting immune cells to foci of infection.

TABLE OF CONTENTS

LIST OF ABBREVIATIONS

ABC transporter	ATP-Binding Cassette
ATP	adenosine-5'-triphosphate
CAS	chrome azurol S
CCR2	CC chemokine receptor 2
CD14	cluster of differentiation 14
CDM	Chamberlain's defined medium
cDNA	complementary DNA
CFU	colony-forming units
CHA	cystine heart agar
Che-CDM	Chelex-100-treated CDM
CSF	colony-stimulating factor
DFO	deferoxamine mesylate
DIP	2,2'-dipyridyl
DNA	deoxyribonucleic acid
ELISA	enzyme-linked immunosorbent assay
ELR	glutamic acid-leucine-arginine
FBS	fetal bovine serum
Feo	ferrous iron transport
fsl	*Francisella* siderophore locus

FupA	Fe utilization protein A
Fur	ferric-uptake regulator
IFN-γ	interferon-γ
igl	intracellular growth locus
IL	interleukin
IRP	iron regulatory protein
JAK-STAT	Janus kinase-signal transducer and activator of transcription
LB	Lysogeny broth
LDH	lactate dehydrogenase
L-NMMA	L-monomethylarginine
LPS	lipopolysaccharide
LVS	live vaccine strain
MAPK	mitogen-activated protein kinase
Mgl	macrophage-growth locus
MH	Mueller Hinton
migR	intracellular growth regulator
MOI	multiplicity of infection
NF-κB	nuclear factor kappa-light-chain-enhancer of activated B cells
NK cell	natural killer cell
NKT cell	natural killer T cell

NOD	nucleotide-binding oligomerization domain
Nos2	inducible nitric oxide synthase
OD	optical density
ORF	open reading frame
PAMP	pathogen-associated molecular pattern
PBS	phosphate buffered saline
pdp	pathogenicity determinant protein
pig	pathogenicity island gene
PRR	pattern recognition receptor
RIG	retinoic acid-induced gene
RNA	ribonucleic acid
rRNA	ribosomal ribonucleic acid
RT-PCR	reverse transcription-polymerase chain reaction
SD	standard deviation
TLR	Toll-like receptor
TNF-α	tumor necrosis factor-alpha
TUNEL	terminal deoxynucleotidyl transferase dUTP nick end labeling

LIST OF FIGURES

LIST OF TABLES

ACKNOWLEDGEMENTS

I am deeply grateful to members of my committee: David G. Thanassi, Howard B. Fleit, James B. Bliska, Jorge L. Benach, and Richard R. Kew. Their insight, support, and encouragement not only make my project go well but also broaden my knowledge in related fields. I thank Patricio Mena, Gloria Monsalve, Hong Wang, Lance Palmer, and Susan Van Horn for their professional technical support and assistance with my experiments. I am thankful to past and present members of the Center for Infectious Diseases for the friendly and kindly environment. I am especially thankful to Gabrielle Platz and Subhra Chakraborty for their help and suggestions to my work. I am appreciative of past and present members of Furie laboratory. I am indebted to Jaime Italo Bhalla, Indralatha Jayatilaka, and Varya Kirillov for their expert support to my work. I am especially thankful to Indra for her thinking of my family all the time. I thank my family and friends for their unlimited trust and support to my graduate study. Last but not least, I am especially grateful to my advisor, Martha Furie, for her vast patience, support, encouragement, wisdom, and care for not only myself but also my family. I would never wind through the project and improve my ability in the past years without Martha's help and support.

INTRODUCTION

I. Tularemia

A. Overview of *Francisella tularensis*

Francisella tularensis, the causative agent of tularemia, is a coccoid or rod-shaped, non-motile, Gram-negative, zoonotic pathogen (124). Of the identified subspecies, *F. tularensis* subsp. *tularensis* (type A) and subsp. *holarctica* (type B) are the most frequent causes of human disease. Type A exists mainly in North America and type B exists on all continents of the northern hemisphere (43, 124). Infection with type B strains is seldom lethal. However, inhalation of as few as 10 colony-forming units (CFU) of virulent type A bacteria can cause severe disease (111), with a fatality rate of 30% to 60% if untreated (36, 82). As a consequence, *F. tularensis* has been designated a Category A agent of bioterrorism by the Centers for Disease Control and Prevention (106). Due to the high mortality associated with tularemia, *F. tularensis* was once developed as a bio-weapon and is still a potential threat to public health if it were to be released intentionally (40). A live vaccine strain (LVS) of *F. tularensis*, which was derived from a type B strain in the former Soviet Union, is attenuated in humans but highly virulent in mice. The LVS is thus a useful tool to study the pathogenesis of tularemia (31, 47). The taxonomy of *Francisella novicida* is under debate, specifically whether it is a species or a subspecies of *F. tularensis*. Although *F. novicida* rarely causes disease in humans, it is pathogenic in mice and more easily manipulated genetically than *F. tularensis* (44).

B. Routes of infection and symptoms of tularemia

As a zoonotic pathogen, *F. tularensis* has a broad range of hosts; it infects over 250 animal species, including mammals, birds, fish, invertebrates, and amoebae (44, 116). Infections in humans generally result from direct contact with infected animals, transmission from deer flies or mosquitoes, or inhalation of contaminated food or water (4, 124). Various routes of exposure lead to six different clinical manifestations, including ulceroglandular, glandular, oculoglandular, pharyngeal, typhoidal, and pneumonic forms. *F. tularensis* also causes fever, ulceration of skin at the site of infection, pain, and joint stiffness (44). If infections are not confined to the sites of entry by the immune system, the organism spreads and causes systemic infection in the spleen, lung, liver, and circulatory system (5, 31, 46).

C. Intracellular lifestyle of *F. tularensis*

F. tularensis has developed mechanisms to replicate within mammalian cells, such as macrophages and hepatocytes (15, 31, 91, 100, 103), where it is shielded from attack by the immune system and able to obtain sufficient nutrients. Interactions of *F. tularensis* with macrophages are the most thoroughly studied. Most *F. tularensis* organisms enter macrophages after engulfment by asymmetric pseudopod loops (28). After entry, the bacteria are arrested in phagosomes for about 2 to 4 h (109). Subsequently, they escape into the cytosol, where they replicate freely (108). Replication of *F. tularensis* in macrophages requires genes of the *Francisella* pathogenicity island, including intracellular growth locus C (*iglC*), *iglD*, *iglA*, pathogenicity determinant protein A

(*pdpA*), *pdpB*, *pdpD*, and a global regulator called macrophage-growth locus A (*mglA*) (68, 71, 86, 110). Intracellular *F. tularensis* LVS stimulates acquisition of iron by murine macrophages via the transferrin receptor 1 and induces host-cell expression of ferrireductase (Steap3), iron membrane transporter Dmt1, and iron regulatory proteins IRP1 and IRP2 (91). Much less is known about the interactions of *F. tularensis* with non-phagocytic cells.

II. Bacterial metabolism of iron

A. Iron as a double-edge sword

Iron is an essential nutrient for almost all forms of life. Under physiological conditions, iron is in either its reduced ferrous form (Fe^{2+}) or oxidized ferric form (Fe^{3+}). The two redox forms of iron are convertible. Either form of iron can be in a high- or low-spin state depending on its ligand environment, making it flexible to incorporate into various proteins as a biocatalyst or electron carrier (12). Iron is involved in various biological processes, including oxygen transport, DNA synthesis, regulation of gene expression, photosynthesis, respiration, and the trichloroacetic acid cycle (7).

Iron is the fourth most abundant element in the Earth's crust. However, almost all the iron in the biosphere is in the ferric form due to the presence of oxygen. Ferric iron is extremely insoluble in water (10^{-18} M at pH 7.0), making it restricted to all living organisms. Thus, organisms must develop mechanisms to solubilize the iron in order to utilize it. On the other hand, excess free ferrous iron is extremely toxic to living beings under aerobic conditions. Through the Fenton reaction, Fe^{2+} catalyzes the conversion of

less-toxic hydrogen peroxide to highly toxic hydroxyl radicals (OH·), which cause damage to DNA and degradation of proteins (125). Thus, in the presence of oxygen in the modern world, iron is both restricted and potentially toxic. Living organisms must tightly control the availability of iron. They not only need to acquire enough iron to support their physiological demands but also have to limit its toxicity.

B. Bacterial pathways for acquisition of iron

Almost all bacteria need to develop mechanisms to obtain iron from the environment. In the case of Gram-negative *Escherichia coli*, each cell contains 10^5 to 10^6 atoms of iron (1). In a culture with a density of 10^9 organisms per ml, each generation consumes about 10^{18} atoms of iron per liter. Thus, *E. coli* needs a concentration of 10^{-7} to 10^{-5} M iron to support its replication. Other bacteria need similar levels of iron for their growth. However, ferric iron is extremely insoluble at pH 7.0 (only 10^{-18} M). To overcome this limitation, bacteria obtain iron from the environment by secreting chelators that can solubilize ferric iron, reducing it to the more soluble ferrous form. In addition, some pathogenic bacteria can directly use iron that is complexed with host molecules, such as heme, hemoglobin, transferrin, and ferritin (Fig. 1).

i. Siderophore-ferric iron pathway

Siderophores are commonly used by both Gram-negative and Gram-positive bacteria to obtain iron (7). They are small molecules (< 1000 daltons) with an extremely high affinity for ferric iron ($K_{aff} > 10^{30}$). Siderophores have diverse structures and bind ferric iron through various ligands, including hydroxamates, α-hydroxycarboxylates, or

catechols. Bacteria synthesize and secrete siderophores in response to low availability of iron. Binding of ferric iron solubilizes it and makes it accessible to the bacteria. In Gram-positive bacteria, the siderophore-ferric iron complex binds to receptors on the membrane and is internalized by permease proteins and ATP-Binding Cassette (ABC) proteins. In Gram-negative bacteria, the siderophore-ferric iron complex is recognized by receptors on the outer membrane (Fig. 1). Receptors are β-barrel proteins that traverse the outer membrane. Passage of the siderophore-ferric iron complex through this channel to the periplasmic region needs energy, which is provided by the electrochemical charge gradient of the inner membrane. The TonB-ExbB-ExbD protein apparatus delivers this energy to aid the uptake of the siderophore-ferric iron complex. With the help of periplasmic binding proteins, the complex is then shuttled to permease proteins and the ABC transporter and internalized. Hydrolysis of ATP provides the energy needed in this step. In the cytosol, the complex dissociates by reduction of the ferric form to the ferrous form, and the siderophores are recycled or degraded (7).

ii. Feo system

In many bacteria, the ferrous iron transport (Feo) system serves as an alternative pathway (55). Some Gram-negative bacteria, such as *E. coli*, *Campylobacter jejuni*, *Yersinia pestis*, and *Helicobacter pylori*, use the Feo system to obtain Fe^{2+} (63, 85, 93, 130). Typically, this system consists of three proteins, FeoA, FeoB, and FeoC, and the genes encoding them are usually in an operon. However, in some organisms FeoA, FeoC, or both are absent. The function of FeoA has not been determined. FeoC is a small DNA

binding protein, likely a transcriptional repressor (24). As the core of the system, FeoB forms a channel on the bacterial inner membrane via its C-terminus, whereas the N-terminus is a G-protein-like domain in the cytosol that is believed to regulate the uptake of ferrous iron (24). The structure of the G-protein-like domain of FeoB of several organisms has recently been determined (59, 62, 94). However, the structure of the transmembrane domain is not known. Thus, the detailed mechanism by which FeoB works is not clear.

The Feo system plays an important role in acquisition of iron in anaerobic conditions, such as in the intestine, where ferrous iron predominates over ferric iron. *E. coli* and *Salmonella feoB* mutants, which are unable to transport ferrous iron, have poorer ability to colonize the mouse gut (119, 127). It is not clear whether the Feo system plays a role in environments where ferrous iron is scarce. Extracellular ferric iron reductase activity has been identified in many bacteria, such as *E. coli* and *H. pylori* (33, 136). Conversion of ferric iron to ferrous iron by this enzyme facilitates the transport of iron through the Feo system.

iii. Acquisition of iron by pathogenic bacteria

Iron in hosts is tightly regulated. In addition to controlling the toxicity of iron, the hosts limit iron availability as part of their innate immune mechanisms. In extracellular niches, mammalian iron-binding proteins, such as transferrin, hemoglobin, and lactoferrin, reduce the concentration of free iron to 10^{-18} M, which is insufficient for bacterial growth (20). When iron is imported into cells, it is reduced to ferrous iron to be incorporated into

enzymes or heme or utilized by other pathways. Excess free iron is either stored intracellularly bound to ferritin in its ferric form or exported through ferroportin to the extracellular environment, where it is oxidized and bound to other proteins (113). Pathogens often use low levels of iron as a signal to turn on virulence genes (77). Some pathogens obtain iron by utilizing siderophores to compete with iron-binding proteins (135). However, other pathogens use receptors to directly obtain iron bound to host proteins or heme (Fig. 1). For example, transferrin and lactoferrin receptors have been indentified in pathogenic bacteria (32). These receptors are located on the outer membrane, where they can recognize holo-transferrin or lactoferrin carrying ferric iron. Upon binding, the iron is removed by the receptors, and the apo-transferrin or lactoferrin is released. Transport of the ferric iron across the outer membrane is TonB-ExbB-ExbD-dependent, and its passage through the periplasm and inner membrane depends on a periplasmic binding protein (called ferric-binding protein) and the ABC/permease apparatus (7).

Heme is the most abundant source of iron in hosts and is mainly contained in red blood cells. Some pathogens, such as *Bacteroides fragilis*, can use heme, hemoglobin, or the hemopexin-heme complex as sources of iron (90). Certain extracellular pathogens employ hemolysins and proteases to lyse red blood cells and release heme or hemoproteins. For Gram-negative bacteria, utilization of heme or heme complexes involves binding of these molecules to receptors on their outer membrane. Some bacteria produce hemophores, which chelate hemoglobin or hemopexin and facilitate their

binding to receptors. Transport of the free heme group across the outer membrane is TonB-ExbB-ExbD-dependent. Internalization of heme requires the ABC transporter. Heme is degraded in the cytoplasm by heme oxygenase, and iron is released.

Intracellular pathogens, such as mycobacteria, *Chlamydia* species, and *Legionella pneumophila*, also depend on host-derived iron. The mycobacteria, including *Mycobacterium avium* and *Mycobacterium tuberculosis*, block the maturation of phagosomes and arrest the phagosomes at an early endosomal stage. The organisms can utilize host iron bound to transferrin in the phagosomes (112). *M. tuberculosis* also can directly use sources of iron in the host cell cytoplasm (89). For some pathogens replicating in the cytoplasm, holoferritin is the main source of iron. For instance, *Neisseria meningitides* living in epithelial cells recruits and aggregates holoferritin. The aggregated ferritin is rapidly degraded, and iron is released (69).

Figure 1. Iron uptake pathways of Gram-negative bacteria.
Under iron-restricted conditions, many bacteria produce siderophores to chelate ferric iron from the environment and internalize the complex by receptors on the outer membrane. Some pathogens produce hemophore, which is a heme-binding protein, or express receptors for heme, hemoglobin, or hemopexin, which can take up heme-iron complexes. Additionally, some pathogens possess receptors for iron-binding proteins of the host, such as lactoferrin and transferrin, and extract iron from them. The internalized iron is transported across the inner membrane in the aid of ABC transporters. In addition, many bacteria have a ferrous iron transport (Feo) system, of which FeoB is a transporter on the inner membrane. FeoB transports ferrous iron across the inner membrane, probably with the aid of certain ferric reductases. The Feo system is not as well-studied as the ferric iron transport systems. Reprinted from Hantke (55) with permission from Elsevier.

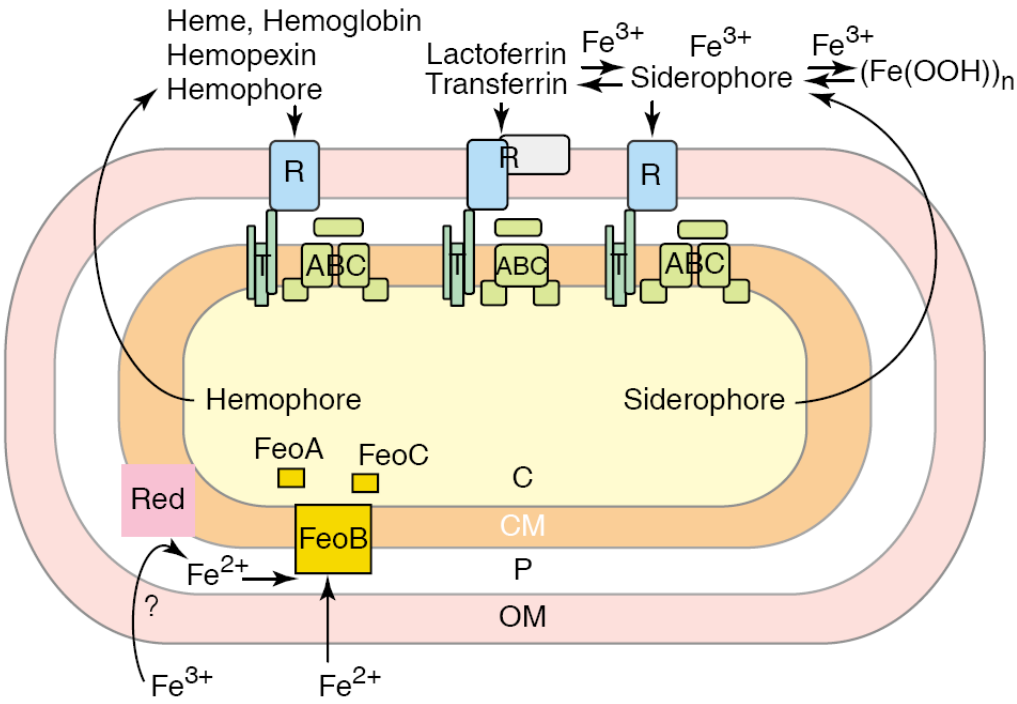

TRENDS in Microbiology

C. Iron in bacteria is tightly regulated

Expression of genes related to iron acquisition is regulated according to the availability of iron. Bacteria must tightly control the amount of iron within to meet their need for iron and to restrict the deleterious effects caused by excess free iron. Bacteria also use low availability of iron as a signal to turn on virulence genes.

Ferric-uptake regulator (Fur) protein is a global repressor of gene expression in many bacteria. Fur regulates gene expression in an iron-dependent way. Ferrous iron is a co-repressor of Fur. Binding of iron to Fur increases the affinity of Fur for its DNA binding site. A Fur binding site (Fur box) is located between nucleotides -35 and -10 in the promoters of Fur-regulated genes. At high levels of iron, Fur together with ferrous iron binds the Fur box to turn off expression of the gene. At low levels of iron, Fur loses ferrous iron, and apo-Fur dissociates from the Fur box, turning on expression of the gene. In *E. coli*, Fur controls expression of over 90 genes, including genes related to biosynthesis and transport of siderophores and storage of iron. Production of siderophores is up-regulated when iron is restricted. Receptors of siderophores are also induced by iron starvation and not present under iron-sufficient conditions. Siderophores and the Feo system have high affinity for iron and are strategies used to overcome limitation of this nutrient. It has not been determined how bacteria acquire iron when iron is plentiful. In *E. coli* and *H. pylori*, low-affinity transport occurs under conditions of iron abundancy, but the pathways are not clear (7, 130).

D. *F. tularensis* and iron

Iron is an essential nutrient for *F. tularensis*. Some media designed at early times for cultivation of *F. tularensis* contained blood or derivatives of blood. Later, it was found that the main role of blood is to provide iron as a nutrient (126). With respect to pathways by which *F. tularensis* obtains iron, the role of the *Francisella* siderophore locus (*fsl*) operon has been investigated previously. The *fsl* operon is composed of six genes (*fslA* to *fslF*). Genes of the *fsl* operon are involved in biosynthesis and probably uptake of siderophores (39, 65, 101, 122). The genes of this operon are the most highly up-regulated when *F. tularensis* LVS grows in iron-restricted conditions (39). FslA is required for production of siderophores in the LVS, the highly virulent type A *F. tularensis* Schu S4 strain, and *Francisella novicida* U112 (39, 122). In *F. novicida* U112, the genes *fslABC* are all required for production of siderophores, but Δ*fslD* and Δ*fslE* mutants secrete siderophores at levels equivalent to the wild-type bacteria. However, deletion of any of these five genes stunts growth of *F. novicida* U112 in iron-restricted media. FslE is identified as an outer-membrane protein (60). Unlike that of other *fsl* mutants, the growth of the Δ*fslE* strain cannot be restored by addition of exogenous siderophores (65). Similarly, a Δ*fslE* mutant of the Schu S4 strain makes but cannot utilize siderophores, leading to the suggestion that FslE may be a receptor for siderophores (101). It is notable that no homologous gene encoding TonB has been identified in the genomes of *F. tularensis* strains. TonB is the major component of the energy transducer of the electrochemical gradient. However, internalization of the

siderophore-ferric iron complex in *F. tularensis* also depends on energy provided by the electrochemical gradient (37).

A gene encoding the Fur repressor and a Fur box are located upstream of the *fsl* operon (39, 65, 101, 122). When iron is abundant, Fur together with ferrous iron (Fe^{2+}) represses the expression of the operon by binding to the Fur box. Under conditions of restricted iron, Fur dissociates from the Fur box. Consequently, expression of the operon and the siderophore-Fe^{3+} uptake pathway is turned on (19, 39, 122). However, elimination of siderophores of the LVS by deletion of the *fslA* gene does not affect its growth in macrophages (39), indicating that the LVS possesses additional pathways to obtain iron in these cells.

A 58-kilodalton protein encoded by FTT0918 in the Schu S4 strain is required for efficient utilization of iron in both siderophore-dependent and -independent manners (76). The LVS, however, does not contain a similar gene. Evidence of another iron acquisition pathway in *F. novicida* was reported by Crosa *et al.* (37). Mutation of the gene FTN_1272, which encodes a putative proton-dependent oligopeptide transporter, results in poorer import of radioactive iron and lower levels of intracellular iron. Genes homologous to FTN_1272 are present in *F. tularensis* Schu S4 (FTT1253) and the LVS (FTL_0691), but their functions have not been studied.

The Feo system is another possible iron transporter in the *F. tularensis* LVS. The genes *feoA* (FTL_0660) and *feoB* (FTL_0133) have been identified in the genome. Unlike the case in *E. coli*, the genes are not in an operon. Inactivation of *feoB* using a

Tn*5*-based transposon-transposase complex attenuates the growth of the mutant in lungs in a murine model of respiratory tularemia (120), but the biological function of FeoB in this bacterium has not been studied in detail.

Genes of the *Francisella* pathogenicity island are required for intracellular growth. As low availability of iron mimics the case in hosts, it is likely that the organism uses limited iron as a signal to regulate gene expression to adapt to niches in its mammalian hosts. Analysis by two-dimensional gel electrophoresis and mass spectroscopy showed that three pathogenicity-island proteins encoded in the *igl* operon, IglA, B, and C, are upregulated when the LVS grows under iron-restricted conditions (74). It has been determined that regulation of the *igl* operon is iron-dependent but Fur-independent. The regulator of the operon is macrophage intracellular growth regulator (migR), encoded by the gene FTL_1542. Mutation of *migR* leads to lower transcription of *iglC*, reduced ability to grow in human macrophages, arrest of the mutant in mature phagolysosomes enriched with both lysosomal-associated membrane protein 1 and cathepsin D, and impaired ability to prevent production of neutrophil oxidants (18).

III. Innate immunity

The innate immune response is the first line of host defense. Innate immunity includes physical and chemical barriers, humoral factors, phagocytic cells, and lymphocytic cells. Tight junctions of epithelial cells and mucosal membranes are examples of the physical barriers. Chemical barriers are set up by the body to kill invading pathogens and include substances such as hydrochloric acid in the stomach.

Humoral factors are soluble molecules in the bloodstream and bodily fluids, and examples are antibacterial peptides, complement proteins, and interferons. Neutrophils and macrophages are the major phagocytic cells. They take up and degrade insoluble particles, such as bacterial pathogens. Macrophages also form an important link between innate immunity and adaptive immunity by presenting antigens to T cells. Lymphocytic cells involved in innate immunity include natural killer (NK) and natural killer T (NKT) cells, which serve key roles in immune regulation by producing various cytokines and chemokines. Activated NK cells also can directly lyse infected cells and tumor cells by producing perforin and proteases (49).

A. Recognition of microbes by the innate immune system

Unlike the adaptive immune response, the innate immune system does not need to be primed to recognize pathogens with full efficiency. The innate immune cells recognize pathogen-associated molecular patterns (PAMPs) through pattern recognition receptors (PRRs) (61). PAMPs are microbial molecules, including proteins, saccharides, lipids, and nucleic acids, that are stable and generally similar among different organisms. This system allows the host to sense the invasion of various pathogens through a low number of receptors. Host PRRs include phagocytic PRRs, secreted PRRs, and membrane-bound or intracellular PRRs (61, 67). The phagocytic PRRs are mannose receptors and scavenger receptors, which play important roles in clearing pathogens. The secreted PRRs are proteins that can kill pathogens through activation of complement and opsonization of pathogens for phagocytosis, such as C-reactive protein,

lipopolysaccharide-binding protein, serum amyloid proteins, and soluble CD14. Membrane-bound or intracellular PRRs include Toll-like receptors, nucleotide-binding oligomerization domain (NOD)-like receptors, and the retinoic acid-induced gene I (RIG)-like helicases (2, 64, 83). They are expressed not only by innate immune cells but also by some endothelial and epithelial cells, allowing wide detection of pathogens. These receptors play important roles in sensing the presence of pathogens and stimulating signaling pathways to induce expression of proinflammatory factors, such as cytokines, chemokines, and adhesion molecules.

B. Cytokines and chemokines

Cytokines are small proteins that function as immunomodulating molecules. They are signaling molecules that mediate cellular communication. Upon binding of a cytokine to its receptor, a signal is transduced to cells to cause altered function and behavior. Various cytokines, their receptors, and different types of cells together form a complicated network, which links the innate and adaptive immune systems together (10, 22). Some of the most important cytokines involved in the immune response are interferon-γ (IFN-γ), tumor necrosis factor-α (TNF-α), and interleukin-1β (IL-1β). IFN-γ is produced by NK cells and T lymphocytes in response to stimulation with IL-12 (13, 14, 134). IFN-γ is important for control of intracellular bacteria. It inhibits replication of various bacteria, including *Francisella tularensis* and *Listeria monocytogenes*, in macrophages or hepatocytes (8, 53, 56, 98, 123). IFN-γ also down-regulates the level of iron in human monocytes and inhibits the intracellular replication of *Legionella*

pneumophila (21). TNF-α and IL-1β are important proinflammatory cytokines, which can be induced during inflammation, injury, and infection (23). Endothelial cells stimulated by TNF-α and IL-1β produce higher levels of adhesion molecules and secrete chemottractants, facilitating recruitment of leukocytes from the bloodstream to foci of injury or infection (129).

Chemokines are a family of cytokines produced by a variety of cells. The name is derived from their function of causing directed chemotaxis of subpopulations of leukocytes. Leukocytes patrol the bloodstream through selectin-mediated, low-affinity, reversible interactions with endothelial cells. Once leukocytic chemokine receptors are engaged, integrins on the leukocytes are activated and induce high-affinity interactions between the integrins and endothelial cell adhesion molecules (102). Immune cells bearing the receptor also will move from lower to higher concentrations of that chemokine (84). Migration of monocytes from the bone marrow to the bloodstream is also mediated by chemokines and their receptors, such as CCR2 (115). Thus, chemokines facilitate the recruitment of certain immune cells from the bone marrow to the bloodstream and/or from the bloodstream to the foci of infection.

According to the spacing of two conserved cysteines near the amino-terminus, chemokines can be classified into three groups (CC, CXC, and CX_3C). Unlike other chemokines, a fourth group of chemokines has only one cysteine near the amino-terminus; thus they are named C chemokines (73, 84). Generally, CC chemokines induce the migration of monocytes and other cell types such as NK cells and dendritic cells. For

instance, CCL2 (also known as monocyte chemoattractant protein-1) induces monocytes to enter the surrounding tissue to become tissue macrophages. CXC chemokines can be further divided into two categories: those with a specific amino acid sequence of glutamic acid-leucine-arginine (ELR) immediately before the first cysteine of the CXC motif (ELR-positive), and those without an ELR motif (ELR-negative). The ELR-positive CXC chemokines, including CXCL1, CXCL2, and CXCL8, specifically induce chemotaxis of neutrophils. The ELR-negative CXC chemokines, such as CXCL9, CXCL10, CXCL11, and CXCL13, are chemottractants for lymphocytes, such as T cells (38). CX_3CL1 is the only member of the CX_3C group. CX_3CL1 is produced in both soluble and transmembrane forms; thus it acts as both a chemokine and an adhesion molecule (66). The C chemokines attract T cell precursors to the thymus. The production of chemokines is induced in various types of cells by different signals, including proinflammatory cytokines and bacterial products such as lipopolysaccharide (LPS) and lipoproteins (45, 87).

C. The role of the liver in innate immunity

i. Components and structure of the liver

The liver can be considered as an organ of innate immunity. The liver receives 80% of its blood supply from the portal vein. This blood is collected from the gut, which contains abundant bacterial products (49). The cellular and humoral composition of the liver allows it to be the first organ to respond to these bacterial products. Hepatocytes compose 70% of the cell number and 80% of the volume of the liver and form the

framework of this organ. Fenestrated endothelial cells line the blood-carrying sinusoids. Kupffer cells (resident macrophages in the liver), NK cells, NKT cells, and dendritic cells reside in the sinusoids, where they have direct contact with endothelial cells or hepatocytes (49). Unlike endothelium in most blood vessels, there is no basal lamina between hepatic endothelium and hepatocytes. Instead, hepatic stellate cells exist underneath some endothelial cells. This structure allows different types of cells in the liver to contact each other, as well as cells passing by in the bloodstream (35). The structure of the liver also permits different cells to access bacterial products, which makes the liver a filter for removal of toxins and pathogens. Hepatic endothelial cells and Kupffer cells are key players for elimination of soluble macromolecules and insoluble waste through endocytosis and phagocytosis (49). In rat and human, the liver contains a high percentage of NK cells, which represent about 30% to 50% of the total lymphocytes in the liver. The hepatic NK cells play an important role in the innate response to tumors, viruses, intracellular bacteria, and parasites (14, 26, 121).

ii. Role of hepatocytes in innate immunity

Hepatocytes also play an essential role in innate immunity in liver. They produce over 80% of complement proteins and secreted PRRs. Expression of genes encoding these proteins is regulated by liver-specific transcription regulators. During infection and inflammation, proinflammatory cytokines, such as TNF-α, IL-1, IL-6, and IFN-γ, induce hepatocytes to produce high levels of these proteins (49). Hepatocytes produce all of the components of the classical and alternative pathways of the complement system, as well

as regulators of this system. The PRRs produced by hepatocytes include C-reactive protein, serum amyloid protein, LPS-binding protein, soluble CD14, and antimicrobial peptides, such as hepcidin (49). Hepcidin is the central regulator of the body's iron metabolism. It is a small peptide hormone, which binds to ferriportin on cellular membranes to block the export of iron from cells. In response to bacterial infection or iron overload, hepcidin reduces the levels of iron in the bloodstream by maintaining it in cells, such as macrophages (48).

Not only are hepatocytes effector cells, but they also are producers of cytokines. In response to treatment with IFN-γ, hepatocytes limit the intracellular growth of *Listeria monocytogenes* (53, 56, 123), *Francisella tularensis* (34), and *Legionella pneumophila* (21). In addition, upon stimulation or bacterial invasion, hepatocytes express a series of proinflammatory cytokines. These include CXC and CC chemokines, as well as TNF-α and macrophage colony-stimulating factor (107).

D. Innate immune response to *F. tularensis* in the liver

i. Pathological changes of the liver in tularemia

No matter what the route of infection, the liver is a target organ if *F. tularensis* is not controlled at the original site of entry. After intravenous inoculation of mice, both Kuppfer cells and hepatocytes are found infected at 16 h. Neutrophils are recruited to the liver at this early time of infection. Infected hepatocytes are lysed extensively at 48 h of infection. Blockade of recruitment of neutrophils permits the replication of *F. tularensis* in hepatocytes, leading to a higher burden of bacteria in the liver and higher susceptibility

of the mice (31). However, it seems that neutrophils by themselves are not enough to control the infection in the liver. After intradermal inoculation with a sublethal dose of the LVS, the ratio of neutrophils to lymphocytes and monocytes in the peripheral blood increases on day 1 and day 2 after infection, but declines to normal levels on days 4 and 5 (103). Immune cells infiltrate into the infected liver and granulomas form, and *F. tularensis* is found within the area of granulomas. Even though some neutrophils can be found in granulomas on day 5 after inoculation, mononuclear cells, with the majority being Mac-1^+ immature myeloid cells and macrophages, dominate the granulomas. Hepatocytes in the granulomatous regions die mainly through necrosis (103). Overall, it appears that neutrophils are recruited and might play important roles at early times of infection. However, as tularemia progresses, mononuclear cells becomes the predominant effector cells in the liver.

ii. Cytokines in the liver during tularemia

Cytokines are important in controlling hepatic infection with *F. tularensis*. In murine tularemia caused by subcutaneous infection with either the LVS or a highly virulent type A strain, expression of IL-12, TNF-α, IFN-γ, and IL-10 is upregulated at 48 h of infection (51, 52). IFN-γ is essential for controlling *F. tularensis* in the liver. IFN-γ is a key factor for regulating the formation of hepatic granulomas and expression of inducible nitric oxide synthase (Nos2) during tularemia (14). IFN-γ-deficient mice have fewer and smaller hepatic granulomas. *F. tularensis* antigens are restricted to granulomas in wild-type mice but disseminated throughout the liver in IFN-γ-deficient mice.

Knockout of IFN-γ also leads to higher numbers of bacteria in the liver and blood. The expression of Nos2 is seen in hepatic granulomas of wild-type mice, but it is absent in the livers of IFN-γ-deficient mice infected with the LVS. Nos2-deficient mice show decreased frequency of granulomas and fewer terminal deoxynucleotidyl transferase dUTP nick end labeling (TUNEL)-positive cells (14), indicating that nitric oxide is involved in destruction of host cells. NK cells are the main source of IFN-γ in the tularemic liver (14, 58). IL-12 and IL-18 appear to be essential inducers of this IFN-γ, as treatment with antibody to IL-12 or IL-18 inhibits production of IFN-γ. Moreover, IL-12-deficient mice do not produce IFN-γ in response to infection with *F. tularensis in vivo* (134). As leukocytes are recruited to the foci of infection in the liver during tularemia, cytokines and chemokines must play important roles in this process. However, except for IFN-γ, the cellular sources of these agents have not been determined.

AIMS OF THE PROJECT

Francisella tularensis, a facultative intracellular bacterium, infects and replicates in macrophages and hepatocytes both *in vivo* and *in vitro*. The interactions between *F. tularensis* and macrophages have been well characterized. However, little is known about those between *F. tularensis* and hepatocytes. The overall goal of this project was to gain more knowledge about the interplay between *F. tularensis* and hepatocytes.

The first specific aim of this project was to determine the factors that allow *F. tularensis* to adapt to life within hepatocytes. Microarray analysis showed that expression of a gene called *fslC* was the most highly up-regulated when the LVS grew in hepatocytes. This gene is part of an operon that had been reported to be involved in production of siderophores (39, 101, 122), but the function of *fslC* had never been examined. I therefore determined whether the *F. tularensis* LVS requires *fslC* to make siderophores and tested the importance of *fslC* for intracellular growth and virulence of the bacterium. These results indicated that *fslC* is needed for the LVS to acquire iron through the siderophore pathway, but they also showed that this pathway is not essential for growth or virulence. Since iron is an indispensible nutrient for F. tularensis, I then searched for an additional pathway for uptake of iron in the bacterium and demonstrated for the first time that FeoB plays such a role.

The second question explored in this project was how hepatocytes respond to infection with *F. tularensis.* In murine tularemia, neutrophils are recruited to foci of infection in the liver at early times, and mononuclear cells predominate in hepatic

granulomas at later phases of infection. However, the contribution of hepatocytes to recruitment of immune cells during tularemia had not been explored. This project, then, aimed to understand whether hepatocytes play a role in sensing infection with *F. tularensis* and how they cooperate with the immune system to combat this pathogen.

MATERIALS AND METHODS

I. Bacterial strains and culture media

The *F. tularensis* LVS (American Type Culture Collection [ATCC] 29684, Manassas, VA) was a generous gift from Dr. Karen L. Elkins, Center for Biologics Evaluation and Research, Food and Drug Administration, Rockville, MD. Frozen stocks of bacteria were prepared as previously described (87). The *F. tularensis* LVS *feoB::*Tn*5* transposon mutant was a kind gift from Dr. Jing-Ren Zhang, Albany Medical College, Albany, NY. For each in vitro experiment, frozen bacteria were thawed and grown on Chocolate II agar (Becton, Dickinson and Co. [BD], Sparks, MD) at 37°C in 5% CO_2 for two to three days. Single colonies were inoculated into the appropriate medium and cultured overnight at 37°C with shaking at 100 rpm till log phase. *E. coli* DH5α (Invitrogen, Carlsbad, CA) was cultured in LB medium (Sigma-Aldrich Chemical Co., St. Louis, MO) supplemented with 100 μg/ml of ampicillin or 50 μg/ml of kanamycin where appropriate. *F. tularensis* strains with plasmids were cultured in Mueller Hinton (MH) II broth (BD) supplemented with 5 μg/ml of kanamycin or 200 μg/ml of hygromycin B. All antibiotics were from Sigma-Aldrich unless otherwise indicated.

II. Mammalian cells and culture media

FL83B (CRL-2390; ATCC) is a hepatocytic cell line derived from the normal liver of a fetal mouse (16). FL83B cells were cultured in F-12K medium (ATCC) supplemented with 10% fetal bovine serum (FBS; HyClone, Logan, UT). The AML12 cell line (CRL-2254; ATCC) was derived from hepatocytes of a mouse transgenic for

human transforming growth factor α (137). The AML12 cells were grown in Dulbecco's Modified Eagle Medium:F-12 (ATCC) supplemented with 5 μg/ml of insulin, 5 μg/ml of transferrin, 5 ng/ml of sodium selenite, 40 ng/ml of dexamethasone, and 10% FBS. HepG2/C3A (CRL-10741; ATCC) is a clonal derivative of the human HepG2 hepatocytic cell line and was grown in Eagle's Minimal Essential Medium (ATCC) containing 10% FBS. HH4 is a human fetal hepatocytic cell line provided by Dr. Nelson Fausto (University of Washington School of Medicine, Seattle, WA) and was cultured in Williams' Medium E (Invitrogen) with supplements as described (138). All media supplements were from Sigma-Aldrich unless otherwise indicated.

Human macrophages were derived from monocytes isolated from peripheral blood of healthy adult donors using the human Monocyte Isolation Kit II (Miltenyi Biotec, Auburn, CA) as described by Bolger *et al.* (15). To prepare human monocyte-derived macrophages, purified monocytes were cultured for 5 days in RPMI Medium 1640 (Invitrogen) supplemented with 10% heat-inactivated (56°C for 30 min) FBS and 50 ng/ml of macrophage colony-stimulating factor (R&D Systems, Inc., Minneapolis, MN). Collection of human blood was approved by the Stony Brook University Committee on Research Involving Human Subjects.

III. Assays of intracellular bacterial growth

To infect host cells, bacteria grown to log phase in MH II broth supplemented with 2% IsoVitaleX Enrichment (BD), 5.6 mM D-glucose, 625 μM $CaCl_2$, 530 μM $MgCl_2$, and 335 μM ferric pyrophosphate were centrifuged at 4,000 × *g* for 10 min, and

the pellet was resuspended in the appropriate cell culture medium to the desired multiplicity of infection (MOI). The number of bacteria was estimated by measuring the optical density at 600 nm (OD_{600}), and the precise number was determined by retrospective plating on Chocolate II agar. About 1.5×10^5 FL83B hepatocytes were seeded into each well of 24-well plates 24 h before infection. Bacteria were added to hepatocytes in tissue-culture wells, and plates were centrifuged at 240 × *g* for 5 min. After incubation at 37°C for the indicated times, the cultures were washed and treated with 5 μg/ml of gentamicin (Invitrogen) for 1 to 24 h to kill remaining extracellular organisms. In some experiments, hepatocytes were treated with 75 μM 2,2'-dipyridyl (DIP; Sigma-Aldrich) for 24 h prior to infection to chelate Fe^{2+} (3, 37, 104). Infection of human macrophages was carried out similarly, but treatment with gentamicin was limited to 1 h; for longer periods of cultivation, antibiotic-free medium was used.

Intracellular bacteria were detected by immunofluorescent staining, CFU assays, and transmission electron microscopy. For visualization by immunofluorescence, infected cells were washed three times with Dulbecco's phosphate buffered saline (PBS; Invitrogen), fixed with 2.5% paraformaldehyde (Electron Microscopy Sciences, Hatfield, PA) in PBS, permeabilized with 0.5% Triton X-100 (Sigma-Aldrich) in PBS for 5 min at 37°C, blocked with 3% bovine serum albumin (Sigma-Aldrich) in PBS for 5 min at 37°C, and stained with rabbit antiserum to the *F. tularensis* LVS and goat anti-rabbit immunoglobulin conjugated to fluorescein isothiocyanate (both from BD). For quantification by CFU assays, the infected cells were lysed with 10 mg/ml of saponin

(Sigma-Aldrich) in PBS for 15 min at 37°C. Cell lysates were diluted in MH II broth and plated on Chocolate II agar, and the number of colonies was determined after incubation at 37°C for 2 to 3 days. The intracellular replication of the LVS was further examined by transmission electron microscopy. Briefly, monolayers of infected or control FL83B or AML12 cells grown on ACLAR® film (Ted Pella, Inc., Redding, CA) were fixed with 2.5% glutaraldehyde (Sigma-Aldrich) and 2.5% paraformaldehyde in PBS, dehydrated, embedded, sectioned, stained with uranyl acetate, and examined on a transmission electron microscope (Tecnai 12 BioTwin G^{02}; FEI Co., Hillsboro, OR) at 80-kV accelerating voltage. Images were obtained using an XR-60 charge-coupled device digital camera system (Advanced Microscopy Techniques Corp., Danvers, MA).

IV. cDNA microarray analysis and real-time reverse transcription-polymerase chain reaction (RT-PCR)

To analyze the transcriptional profile of *F. tularensis* within hepatocytes, cDNA microarrays were used. The *F. tularensis* microarrays, covering 2073 and 1804 open-reading frames of the LVS and type A Schu S4 strain genomes, respectively, were provided by the Pathogen Functional Genomics Resource Center at the J. Craig Venter Institute, Rockville, MD, which is sponsored by the National Institute of Allergy and Infectious Diseases. FL83B cells were grown to confluence on 150-mm dishes and incubated with the LVS at an initial MOI of 150 for 24 h. Cultures then were washed, and incubation was continued for another 24 h in the presence of 5 μg/ml of gentamicin. Bacteria were released from the hepatocytic cells with 10 mg/ml of saponin, 19% (v/v)

ethanol, and 1% (v/v) phenol in water, along with vigorous pipetting and vortexing of the suspension. Hepatocytic debris was removed by centrifugation at 1,000 × *g* at 4°C for 5 min. Bacteria were pelleted by centrifugation at 10,000 × *g* at 4°C for 20 min. Total bacterial RNA was isolated using the RNeasy Midi Kit (Qiagen, Valencia, CA). The LVS organisms grown to log phase in MH II broth overnight at 37°C and in the presence of 5% CO_2 were processed identically for comparison. cDNA was synthesized and microarrays were processed as described by Bakshi *et al.* (9). The microarray data were analyzed with the Limma module (118) of the Bioconductor package (50) for the R statistical environment. Four experiments were performed, with dye-swaps applied between each two experiments to eliminate any possible dye bias.

To verify the microarray data, the same RNA samples were subjected to real-time RT-PCR to assess levels of expression of *fslA* and *fslC*. The total RNA was reverse-transcribed into cDNA using Qiagen's QuantiTech® Reverse Transcription Kit with random hexamers (Qiagen) as the RT primers instead of the primer mix in the kit. Assays were performed in the 7500 Real Time PCR System (Applied Biosystems, Carlsbad, CA) using SYBR® Green as the detector (QuantiTech® Primer Assays; Qiagen). Primers for *fslA* were Primers 1 and 2, and primers for *fslC* were Primers 3 and 4 (Table 1). The expression of the 16S rRNA gene was used as an endogenous control (Primers 5 and 6). Relative quantification of gene expression was determined according to the method of Pfaffl (97).

V. Construction of gene deletion mutants of the *F. tularensis* LVS

To produce an in-frame deletion of *fslC*, two fragments within the gene were amplified using the Expand High Fidelity PCR System (Roche Diagnostics, Indianapolis, IN). Primers for the upstream fragment were Primers 7 and 8 (Table 1). Primers for the downstream fragment were Primers 9 and 10. Both fragments were purified from agarose gels using the QIAquick® Gel Extraction Kit (Qiagen), inserted into the pGEM®-T Easy vector (Promega, Madison, WI), and amplified in *E. coli* DH5α. The fragments were purified by digesting the plasmids from *E. coli* DH5α with Sal I and Nde I and inserted at the Sal I site of the suicide plasmid pMP590 (a gift from Dr. Martin S. Pavelka, Jr, University of Rochester Medical Center, Rochester, NY). Primers 11 and 12 on each side of the Sal I site on pMP590 were used to verify the correct insertion of up- and downstream fragments. The portion of *fslC* between the upstream and downstream fragments was deleted through allelic exchange using the pMP590 suicide vector as described by LoVullo *et al.* (79). Primers 13 and 14 within the deleted fragment were employed to confirm the success of the procedures. RT-PCR with Primers 15 and 16 specific for *fslB* and Primers 17 and 18 specific for *fslD* was performed and demonstrated that the in-frame deletion of *fslC* did not affect the expression of these adjacent genes. A complementing plasmid encoding *fslC*, with the shuttle vector pMP633 (a gift from Dr. Martin S. Pavelka, Jr) as the backbone, was constructed and introduced into the Δ*fslC* strain by electroporation (79). To optimize expression of *fslC*, a 518-nucleotide fragment covering part of the *fslA* gene and its upstream sequence was cloned as the promoter

region using Primers 19 and 20. Another 1529-nucleotide fragment covering the full length of *fslC* and short up- and downstream sequences also was cloned using Primers 21 and 22. Mlu I (acgcgt) and Nde I (catatg) restriction sequences were included as indicated (Table 1). The two fragments were linked together and inserted at the Mlu I site of pMP633. The correct orientation of insertion was verified using Primers 23 and 24 on each side of the Mlu I site on pMP633. In-frame deletion of *feoB* was carried out in a similar way as for *fslC*. The upstream fragment was cloned using Primers 25 and 26, and the downstream fragment was cloned using Primers 27 and 28. The up- and downstream fragments were linked via a Nde I sequence and were inserted into pMP590 between BamH I and Sal I sites. Primers for the deleted fragments were Primers 29 and 30. A complementing plasmid was constructed by inserting the *feoB* gene and its natural promoter, cloned by Primers 31 and 32, into pFNLTP6 (81) between Nde I and BamH I sites. This plasmid was a kind gift from Dr. Thomas Zahrt (Medical College of Wisconsin, Milwaukee, WI).

VI. Targeted inactivation of *feoB* of the LVS by a group II intron

Insertion of a group II intron (TargeTron) into a gene disrupts expression of the gene. A plasmid (pKEK1140) for insertion of a group II intron into genes of *F. tularensis* was designed and generously provided by Dr. Karl E. Klose (University of Texas San Antonio, San Antonio, Texas) (105). Primers specific for inactivation of *feoB* were purchased from Sigma-Aldrich and designed according to the manufacturer's instructions. A plasmid specific to *feoB* (pKEK1140-*feoB*) was constructed using these primers, and

feoB then was inactivated by insertion of an intron between the 375th and 376th nucleotides as previously described (105). The primers used in this study were 375|376s-IBS (Primer 33), 375|376s-EBS1d (Primer 34), 375|376s-EBS2 (Primer 35), and EBS universal (Primer 36). Another two primers (Primers 37 and 38) were designed to test the correct insertion of the group II intron (Table 1).

VII. Growth of bacteria in iron-replete and iron-restricted media

The MH II broth in which we routinely cultured *F. tularensis* (designated hereafter as MH+) is rich in iron due to supplementation with IsoVitaleX and 335 μM ferric pyrophosphate. However, the LVS grew equally well in MH II broth supplemented only with IsoVitalex (designated as MH-). To limit the availability of Fe^{2+} in MH- broth, 100 μM DIP was added to create MH-/DIP. Similarly, the chelator deferoxamine mesylate (DFO; Sigma-Aldrich) was added to a concentration of 90 μM to make MH-/DFO, in which availability of Fe^{3+} was restricted (39, 99, 131). Bacterial strains were cultured in MH+ overnight to approximately the same OD_{600} and washed in PBS. Equal numbers of each strain then were inoculated into MH+, MH-, MH-/DIP or MH-/DFO, as confirmed by retrospective plating.

Chamberlain's defined medium (CDM) was prepared as previously described (25, 27). To prepare Chelex-100-treated CDM (Che-CDM) with defined levels of iron, CDM lacking $FeSO_4$ and $MgSO_4$ was treated twice with 1% (w/v) Chelex-100 (sodium form; Bio-Rad Laboratories, Hercules, CA) overnight with stirring, and the beads were removed by filtration (76). The medium then was supplemented with essential divalent

cations (550 μM $MgSO_4$, 1.5 μM $ZnSO_4$, 0.2 μM $CuCl_2$, 1 μM $MnCl_2$, and 5 μM $CaCl_2$). Che-CDM was prepared with highly-purified water and stored in plastic bottles to avoid any contamination with iron. Che-CDM supplemented with 7.2 μM $FeSO_4$ is considered to be replete with iron; that with 360 nM or 720 nM $FeSO_4$ is considered to have restricted iron (122). Bacteria from Chocolate II plates were cultured in Che-CDM replete with iron overnight to approximately the same OD_{600} and washed three times with PBS. The OD_{600} of suspensions of various bacterial strains were adjusted to precisely the same level, and 200 μl of each suspension were inoculated into Che-CDM with defined concentrations of iron.

VIII. Measurement of siderophores

Chrome azurol S (CAS; Sigma-Aldrich) assays were adapted to a 96-well microtiter plate format as well as an agar plate format as previously described (114). To detect siderophores in Che-CDM with defined levels of iron, 100 μl of media conditioned by bacteria were mixed with 100 μl of CAS reagent and 2 μl of shuttle solution (114). The OD_{630} was read after 1 h of incubation at room temperature. In some experiments, specific siderophore activity was obtained by normalizing to the bacterial densities (OD_{600}). The agar plate format incorporated the CAS reagent into CDM agar. In this assay, any siderophores produced by the bacteria remove ferric iron from the CAS-Fe^{3+} complex, changing the color of the CAS dye from blue to orange. If bacteria grown on CAS plates produce siderophores, orange halos will form around the colonies.

IX. Intranasal infection of mice

Frozen bacterial stocks were thawed, plated on cystine heart agar (CHA) plates, and cultured at 37°C with 5% CO_2 for 30 to 36 h. CHA plates were prepared from cystine heart agar enriched with hemoglobin (Hemoglobin Solution 2%) according to the instructions of the manufacturer (BD). Bacteria scraped from the plates were washed in PBS and resuspended in MH+ with 10% sucrose. Bacterial suspensions were frozen at -80°C and diluted to the proper MOI at the time of infection. The quantities of bacteria in the dilutions were confirmed by plating on Chocolate II agar plates. Female C3H/HeN mice (Charles River Laboratories, Wilmington, MA) from 6 to 8 weeks of age were housed in dust-free, micro-isolator cages with free access to food and water. Mice were anesthetized by intraperitoneal injection of 100 µl of saline containing 1 mg of ketamine (Fort Dodge Animal Health, Fort Dodge, IA) and 100 µg of xylazine (Ben Venue Laboratories, Bedford, OH) for each 10 grams of body weight. Mice then were infected intranasally with 5×10^5 bacteria in 20 µl of MH+ with 10% sucrose. Experiments with mice were approved by Stony Brook University's Institutional Animal Care and Use Committee.

X. Lactate dehydrogenase (LDH) assay

LDH is an intracellular enzyme in various organisms and is released when cells lyse. Thus, the LDH activity in conditioned medium indicates the percentage of cells that died due to infection with the LVS. Because serum contains LDH, the concentration of FBS in the medium was reduced to 5% for this assay. Murine FL83B or AML12

hepatocytic cells grown to confluence in 24-well plates were infected with the LVS at an initial MOI of 150 for 24 h. The extracellular bacteria were removed, and the cells were incubated in fresh medium for an additional 24 h or 48 h. The conditioned media of infected or uninfected cells were collected and centrifuged to remove any residual cells, and the LDH activities were assayed using the CytoTox 96® Non-Radioactive Cytotoxicity Assay (Promega Corporation, Madison, WI). Aliquots of cell culture medium were incubated in the same way and served as negative controls. A set of uninfected cells incubated in parallel was frozen at -80°C and thawed. The supernatants collected from these cells were centrifuged and used to determine the total cellular content of LDH.

XI. cDNA microarray analysis of the gene expression profiles of hepatocytes infected with *F. tularensis*

To determine the gene expression profiles of hepatocytic cells infected with the LVS at various times, cDNA microarray analysis was performed. The Mouse Exonic Evidence Based Oligonucleotide (MEEBO) arrays developed by a group of researchers from Stanford and University of California, San Francisco were printed by the laboratory of Dr. Bruce Futcher at Stony Brook University. The oligonucleotide set consists of 38,784 70mer probes covering almost 25,000 mouse genes and also includes negative and positive controls (http://www.microarray.org/sfgf/meebo.do). Murine AML12 hepatocytic cells grown to confluence in 6-well plates were infected with the LVS at an initial MOI of 10,000 for 2 h or an initial MOI of 1,000 for 6 h, 12 h, and 24 h. After infection, the

extracellular bacteria were removed, and infected and uninfected cells were treated with RNAlater (Applied Biosystems, Carlsbad, CA) to stabilize RNA molecules. The treated cells were scraped from the plates, and total RNA was isolated with an RNeasy Midi kit (Qiagen). Aminoallyl-dUTP was incorporated into oligo-dT-primed cDNA derived from the total RNA. The cDNA then was labeled with Cyanine 3 or 5 fluorescent molecules. Microarrays were processed and data were analyzed as previously described (9). At least two experiments were performed at each time point, with dye-swaps applied between each two experiments to eliminate any possible dye bias.

XII. Enzyme-linked immunosorbent assay (ELISA) of cytokines and chemokines

To assess production of cytokines and chemokines by infected hepatocytes, murine FL83B or AML12 hepatocytic cells grown to confluence in 24-well plates were infected with the LVS at an initial MOI of 1,000 for 4 h or 24 h. Some cells were treated with a sham preparation of bacteria, which consisted of uninoculated MH II broth subjected to all of the same manipulations as the bacteria themselves. The conditioned media of infected cells, uninfected cells, and sham-treated cells were collected and clarified by centrifugation. Concentrations of CCL5, CCL20, CXCL2, colony-stimulating factor 3 (CSF3), and TNF-α were determined with ELISA kits (R&D Systems, Inc., Minneapolis, MN).

XIII. Production of nitric oxide by infected hepatocytes

Nitric oxide is an unstable, diffusible, small molecule. Nitric oxide produced within cells diffuses into the medium and forms nitrate, which is stable. Nitrate in the

conditioned medium can be reduced to nitrite, and the total concentration of nitrite can be chemically determined. Murine AML12 cells grown to confluence in 24-well plates were infected with the LVS at an initial MOI of 1,000 for 6 h, 12 h, or 24 h. The conditioned media of infected, uninfected, and sham-treated cells were collected and centrifuged to remove any cellular debris. The concentration of total nitrite in the conditioned media was determined with a Total Nitric Oxide Assay Kit (Endogen® Pierce Biotechnology, Inc., Rockford, IL). In other experiments, the production of nitric oxide was blocked using L-monomethylarginine (L-NMMA), an inhibitor of Nos2 (70). AML12 cells were infected with the LVS at an initial MOI of 1,000 for 2 h, and then the extracellular bacteria were removed. The cells were incubated in fresh medium with gentamicin for an additional 1 h, 6 h, 10 h, or 24 h. AML12 hepatocytes were treated with 1 mM L-NMMA during the process of infection and the subsequent period of incubation. At each time point, the amount of viable bacteria in L-NMMA-treated and control cells was determined by CFU assay.

XIV. Treatment with IFN-γ inhibits intracellular growth of *F. tularensis*

To determine the effect of IFN-γ on intracellular growth of the LVS, about 1.5×10^5 AML12 cells were seeded in each well of 24-well plates 24 h before treatment with IFN-γ. Cells were treated with 100 ng/ml of IFN-γ beginning 24 h prior to infection, with infection, or 24 h after infection. In all cases, IFN-γ remained present until the end of the experiment. Control and IFN-γ-treated cells were infected with the LVS for 24 h at an initial MOI of 1,000, and the extracellular bacteria were removed. The cells were

incubated with gentamicin for an additional 24 h. The amount of viable intracellular bacteria was determined by CFU assay.

XV. Statistics

The log-rank test was used to analyze survival of infected mice. Statistical significance of all other data was determined using an unpaired analysis of variance and the Tukey-Kramer multiple-comparisons test (Instat version 3.01, GraphPad Software, San Diego, CA).

Table 1: Primers used in this work

Primer No.	Sequences[a]
1	5'-GCAAGCTGAGCATATTCTCCCAG-3'
2	5'-CACTTGTAGCATGAATTGCCACTG-3'
3	5'-CGAGATTTACCGCAATGGC-3'
4	5'-GCTTAGAGTAGGGCTTATTCCTGC-3'
5	5'-TGGACCGATACTGACACTGAGG-3'
6	5'-AGAGCCTTTACACCGACTCC-3'
7	5'-AGACgtcgacTGCTTCGCCATGCTTTATCATC-3'
8	5'-AGACcatatgCCAATATGACAATGTAGCCCAGC-3'
9	5'-AGACcatatgTGAGCTAGGACGTAGTTTGGTCG-3'
10	5'-AGACgtcgacCTTGGCTTTAGATGGATGAACTCG-3'
11	5'-CCTATGGAAAAACGCCAGCAAC-3'
12	AATACGCAAACCGCCTCTCC-3'
13	5'-TCGAGATTTACCGCAATGGC-3'
14	5'-TCGCTTAGAGTAGGGCTTATTCCTG-3'
15	5'-TGCTTTTCTCTCCTTTTTGGGG-3'
16	5'-GCTGCTATGATTATCGGGTCTGAG-3'
17	5'-GCCACTATCTGAAATCTATGGTCGC-3'
18	5'-CGAGTCCTTGAACAAAACGCC-3'
19	5'-AGACacgcgtGCAGATTGTTGAATCATTCGGTGC-3'
20	5'-AGACcatatgTTTACCAAGAAGCCCCTCACG-3'
21	5'-AGACcatatgGAAATCTCTGTGGCATTTTCCTGG-3'
22	5'-AGACacgcgtGGCAGCAAGAAATATACGCCC-3'
23	5'-GGAGCCTATGGAAAAACGCC-3'
24	5'-GGAGAGCCTGAACCTTTGAAGC-3'
25	5'-ggatccGCTCTAGTTGGCAATCCAAACTGC-3'
26	5'-catatgACCAATACCTTTTGCTGCAACGACT-3'
27	5'-catatgACACTTGCTAAAGAGGTTGTAGTCGG-3'
28	5'-gtcgacGCAGCCAGTAAGATTTGCCACG-3'
29	5'-TGATATTGGTAGTCTGTGGCTTGC-3'
30	5'-CATTTGCGAGAATACCTGTGACAG-3'

31	5'-AGTCcatatgCAGGAACTCAAATCAAGGTATGTAAGG-3'
32	5'-AGTCggatccCGCCTGATTCGCTTTTATTACGACATTTC-3'
33	5'-AAAActcgagATAATTATCCTTAAATAACAAAGGAGTGCGCCCAGATAGGGTG-3'
34	5'-CAGATTGTACAAATGTGGTGATAACAGATAAGTCAAAGGACTTAACTTACCTTTCTTTGT-3'
35	5'-TGAACGCAAGTTTCTAATTTCGGTTTTATTCCGATAGAGGAAAGTGTCT-3'
36	5'-CGAAATTAGAAACTTGCGTTCAGTAAAC-3'
37	5'-CTTGGGCTACCAGTCATATTAGTGG-3'
38	5'-CCAATACCTTTTGCTGCAACGAC-3'

[a]The following restriction sequences are indicated in lower-case letters: Sal I: gtcgac; Nde I: catatg; MluI: acgcgt; BamH I: ggatcc; Xho I: ctcgag.

RESULTS

I. The *Francisella tularensis* LVS grows in hepatocytes

It has been reported previously that *F. tularensis* replicates in murine hepatocytes in vivo (31, 103, 133) and in the human HepG2 hepatocytic cell line (100). To determine whether hepatocytic cell lines generally support growth of the *F. tularensis* LVS, its replication was evaluated in two well-established murine lines, FL83B and AML12, and two human lines, HepG2/C3A and HH4. The hepatocytic cells were incubated with the LVS at an initial MOI of 150 for 24 h. Extracellular bacteria then were washed away, and incubation was continued for another 24 h in fresh medium with gentamicin to kill any remaining extracellular organisms. Visualization of intracellular bacteria in murine FL83B hepatocytes by fluorescence microscopy revealed that cells became infected during the first 24 h of co-incubation, but relatively small amounts of intracellular bacteria were observed (Fig. 2A). However, the number of intracellular bacteria increased greatly after an additional 24 h of culture (Fig. 2B). Human HH4 cells also became infected after 24 h of incubation with the LVS (Fig. 2C), and extensive replication of intracellular bacteria was observed after culture for an additional 24 h (Fig. 2D). Electron microscopy showed small numbers of bacteria in FL83B cells after 24 h of infection (Fig. 2E). Some bacteria appeared to be free in the cytosol, while others were in vacuoles with intact or broken membranes (Fig. 2E, inset), suggesting that the bacteria were escaping from vacuoles into the cytosol. The intracellular bacteria replicated to large numbers, apparently free in the cytosol, over the ensuing 24 h (Fig. 2F). To quantitate replication of

the intracellular organisms, FL83B cells were incubated with the LVS at a MOI of 1,000 for 2 h. Cultures then were washed, and incubation was continued in the presence of gentamicin. At various times, cells were lysed, and the amounts of viable bacteria were determined using CFU assays. The number of viable intracellular bacteria increased about three logs over 30 h (Fig. 3). Fluorescence microscopy and CFU assays showed that the LVS also infected and grew well in murine AML12 and human HepG2/C3A hepatocytic lines (data not shown). The ability to support growth of the LVS thus appears to be shared by several well-characterized murine and human hepatocytic cell lines.

Figure 2. Hepatocytes support the intracellular growth of *F. tularensis*.
Murine FL83B cells (A, B, E, and F) or human HH4 cells (C and D) were incubated with the LVS at an initial MOI of 150 for 24 h, and the extracellular bacteria were removed. The cells then were fixed for visualization immediately (A, C, and E) or after an additional 24-h incubation (B, D, and F). Panels A to D are merged phase-contrast and immunofluorescent images in which the bacteria appear green (original magnification, 400×). Panels E and F are images obtained by transmission electron microscopy. (E) The arrows indicate bacteria that appear to be free in the cytosol at 24 h post-infection, and the arrowheads indicate bacteria that appear fully or partially enclosed by membranes. The inset in Panel E shows a higher-magnification view of two organisms surrounded by a partially disrupted membrane. (F) After 48 h of infection, almost all of the bacteria appear to be in the cytosol, as opposed to surrounded by membranes. Scale bars in Panels E and F, 500 nm.

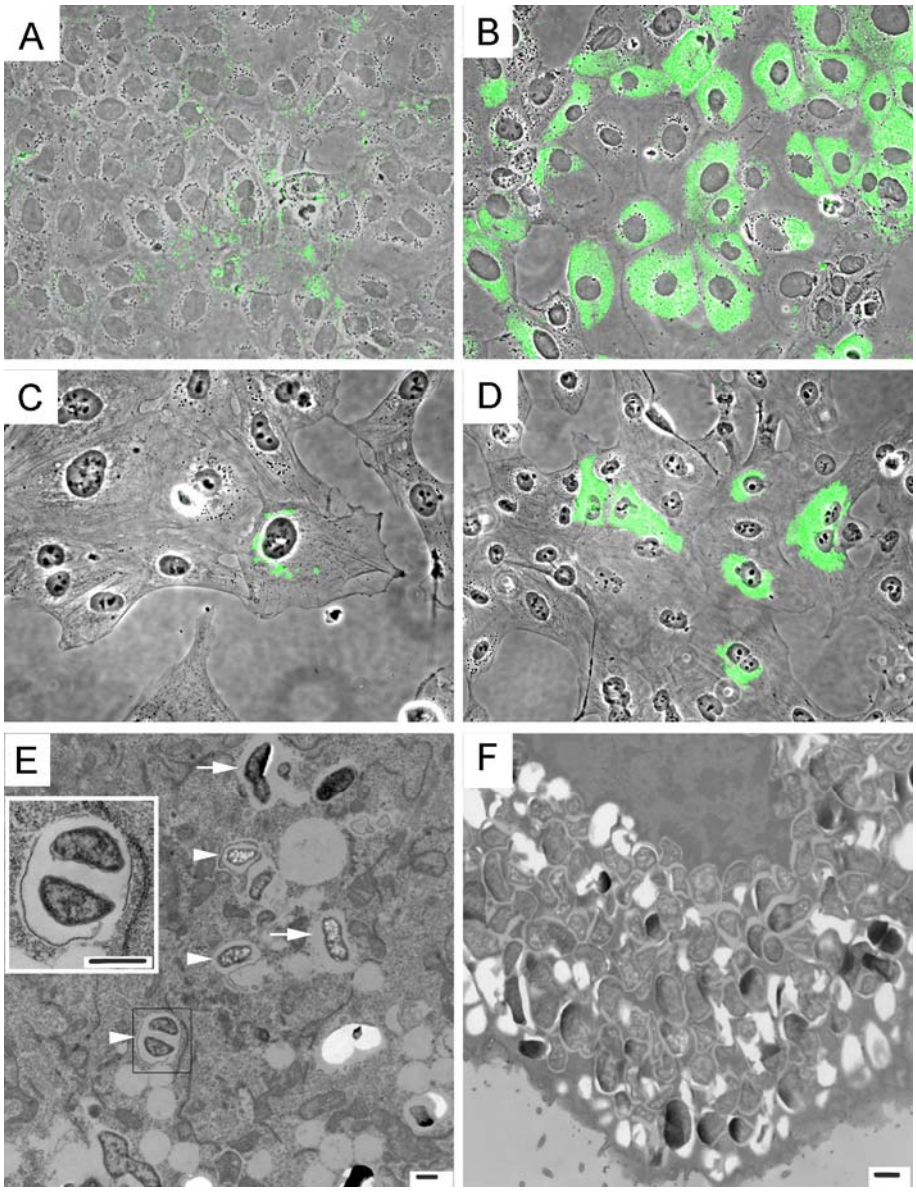
A
B
C
D
E
F

Figure 3. The *F. tularensis* LVS replicates extensively in hepatocytes.
FL83B hepatocytic cells were incubated with the LVS at a MOI of 1,000 for 2 h, extracellular bacteria were removed, and the cells were cultured in medium with gentamicin for the indicated times. Hepatocytes were lysed, and the amounts of viable bacteria were determined by a CFU assay. Data are the means ± SD of three replicate samples. This experiment was repeated twice more with similar results.

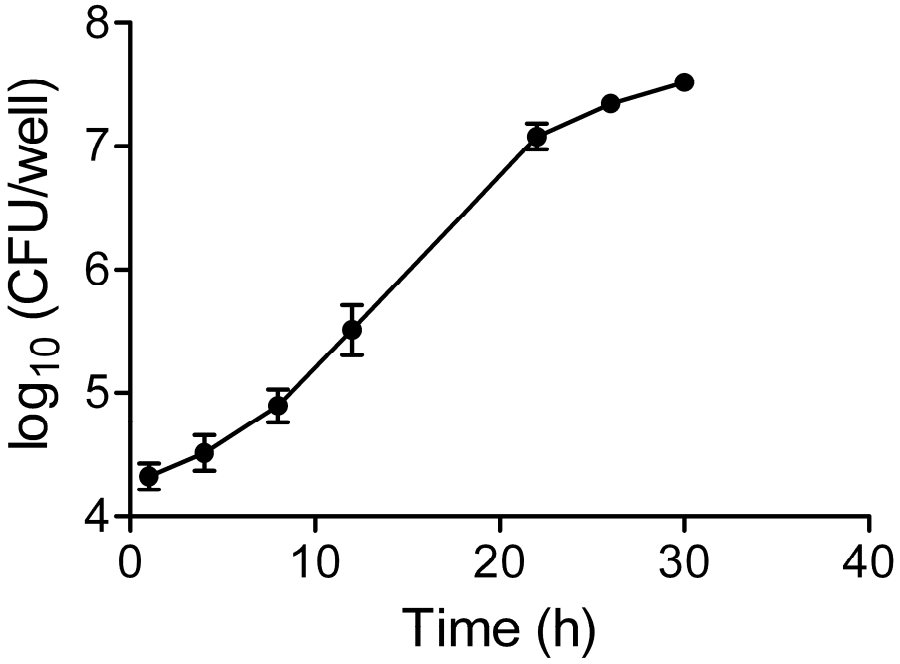
8
7
6
5
4
log10 (CFU/well)
0
10
20
30
40
Time (h)

II. Characterization of iron acquisition pathways of the *Francisella tularensis* live vaccine strain

A. The transcriptional profile of the *F. tularensis* LVS growing in hepatocytic cells is different from that of bacteria cultured in broth

The global gene expression profile of the LVS growing in hepatocytes was assessed to gain insight into how the bacterium adapts to this intracellular niche. Murine FL83B hepatocytic cells were incubated with the LVS for 24 h, washed, and cultured in fresh medium with gentamicin for an additional 24 h. The intracellular bacteria then were released by selective lysis of the hepatocytes. Total RNA was isolated from the intracellular bacteria or bacteria grown in MH+, and the expression patterns were compared using cDNA microarrays. Data averaged from four independent hybridizations showed that expression of 53 genes was up-regulated and that of 20 genes was down-regulated more than two-fold in intracellular bacteria, as compared to bacteria cultured in MH+ (Table 2). Most of these genes encode hypothetical proteins with unknown functions. Most are also present in the genomes of both the LVS and the highly virulent, type A Schu S4 strain. Twelve of the 17 *Francisella* pathogenicity island genes were up-regulated from 2.0- to 5.0-fold, including pathogenicity island gene G (*pigG*), *iglD*, *pigB*, *pigI*, *pigA*, *pigD*, *pdpC*, *pigC*, *pdpA*, *pigH*, *pdpD*, and *pdpB*. Other pathogenicity island genes also were up-regulated but to a lesser extent, including *pigE* (1.8-fold), *iglC* (1.6-fold), *iglB* (1.8-fold), and *iglA* (1.8-fold). Genes encoding MglA and MglB, which regulate expression of virulence genes and are required for growth in

macrophages (11, 17, 71, 110), were down-regulated approximately 2-fold. Four genes of the *fsl* operon, *fslA*, *B*, *C*, and *D,* were the most highly up-regulated, ranging from 6.7-fold for *fslB* to 13.1-fold for *fslC*. Using 16S rRNA as an endogenous control, the up-regulation of *fslA* and *fslC* in intracellular bacteria was verified by real-time RT-PCR, with fold-changes in mRNA levels of 33.3 ± 12.7 and 20.2 ± 5.8, respectively. Similarly, expression of the *fsl* operon is upregulated when the type A *F. tularensis* Schu S4 strain grows in primary human macrophages (132).

Table 2: Up- and down-regulated genes of the LVS grown in FL83B hepatocytic cells for 48 h in comparison with the LVS grown in MH II broth

ORF in LVS[a]	ORF in Schu S4[a]	Product	Symbol	P-Value	Fold Change
FTL_1834	FTT0027c	diaminopimelate decarboxylase	*fslC*	4.4E-10	13.1
FTL_1832	FTT0029c	hypothetical protein	*fslA*	3.8E-08	10.6
FTL_1835	FTT0026c	hypothetical protein	*fslD*	5.4E-10	9.1
FTL_1833	FTT0028c	hypothetical protein	*fslB*	5.1E-06	6.7
FTL_1164	FTT1707	hypothetical protein	*pigG*	3.1E-09	5.0
FTL_0675	FTT1388	hypothetical protein		3.1E-09	4.1
FTL_0953	FTT0677c	hypothetical protein		5.4E-10	3.8
FTL_1218	FTT0981	hypothetical protein		1.2E-06	3.6
FTL_1160	FTT1711c	intracellular growth locus, subunit D	*iglD*	2.6E-07	3.6
FTL_0816	FTT1140	hypothetical protein		3.2E-10	3.5
FTL_0867	FTT0602c	hypothetical protein		1.4E-06	3.5
FTL_0207	FTT0296	Pyrrolidone-carboxylate peptidase	*pcp*	1.5E-07	3.5
FTL_1169	FTT1702	hypothetical protein	*pigB*	2.1E-07	3.4
FTL_0473	FTT0403	peptide deformylase	*def1*	1.5E-08	3.3
FTL_1161	FTT1710	hypothetical protein	*pigI*	7.4E-05	3.1
FTL_1170	FTT1701	hypothetical protein	*pigA*	1.9E-05	3.0
FTL_0026	NA[b]	3-hydroxyisobutyrate dehydrogenase		6.1E-10	3.0
FTL_1217	NA[b]	hypothetical protein		2.3E-05	2.9
FTL_0815	NA[b]	PRC-barrel		3.0E-07	2.9
FTL_1231	FTT0970	hypothetical protein		5.3E-07	2.9
FTL_0449	FTT0383	hypothetical protein		1.2E-06	2.8
FTL_1678	FTT0101	conserved membrane hypothetical protein		7.5E-06	2.8
FTL_1228	FTT0973	hypothetical protein		2.2E-07	2.8
FTL_1167	FTT1704	hypothetical protein	*pidD*	2.0E-08	2.7
FTL_1162	FTT1709	hypothetical protein	*pdpC*	2.5E-03	2.7
FTL_1168	FTT1703	conserved hypothetical protein	*pigC*	2.6E-06	2.7
NA[b]	FTT1143	hypothetical protein		3.4E-06	2.7
FTL_1219	FTT0980	hypothetical protein		5.0E-04	2.6
FTL_1230	FTT0971	cysteine desulfurase activator complex subunit SufB	*sufB*	1.2E-06	2.5

FTL_1172	FTT1699	hypothetical protein	*pdpA*	1.2E-06	2.5
FTL_1163	FTT1708	hypothetical protein	*pigH*	2.6E-05	2.5
FTL_1154	NA[b]	pseudogene		1.9E-07	2.5
NA[b]	FTT1143	hypothetical protein		4.7E-07	2.4
FTL_1755	FTT0133	glycerol uptake facilitator protein	*glpF*	1.3E-08	2.4
FTL_1229	FTT0972	ABC transporter, ATP-binding protein	*sufC*	2.2E-06	2.4
FTL_0924	NA[b]	proton-dependent oligopeptide transporter		1.0E-06	2.4
FTL_1016	FTT0558	short chain dehydrogenase		3.9E-06	2.4
FTL_0663	FTT1400c	hypothetical protein		1.8E-02	2.3
FTL_1503	FTT0720c	deoxyguanosinetriphosphate triphosphohydrolase	*dgt*	2.3E-05	2.3
FTL_1790	FTT0070c	major facilitator superfamily (MFS) tranport protein	*ampG*	2.2E-04	2.2
FTL_0348	NA[b]	pseudogene		1.2E-06	2.2
FTL_0569	FTT1542c	outer membrane protein		5.8E-04	2.2
FTL_1709	FTT1639c	hypothetical protein		5.4E-07	2.2
FTL_0456	FTT0390c	30S ribosomal protein S21	*rpsU*	3.4E-03	2.2
FTL_0217	FTT0306	fumarate hydratase, Class II	*fumC*	2.1E-07	2.1
FTL_0208	FTT0297	hypothetical membrane protein		4.5E-04	2.1
NA[b]	FTT0421	pseudogene		5.7E-04	2.1
FTL_1509	NA[b]	D-alanyl-D-alanine carboxypeptidase/D-alanyl-D -alanine-endopeptidase	*dacB2*	1.4E-05	2.1
FTL_1603	FTT0461	RNA-binding protein	*yhbY*	1.9E-06	2.0
FTL_1601	FTT0463	tRNA/rRNA methyltransferase	*yibK*	2.6E-05	2.0
FTL_1156	FTT1715c	hypothetical protein	*pdpD*	4.4E-05	2.0
FTL_1171	FTT1700	hypothetical protein	*pdpB*	1.4E-02	2.0
NA[b]	FTT0852	pseudogene		3.1E-04	2.0
FTL_1184	FTT1276	macrophage growth locus, subunit B	*mglB*	5.9E-05	-2.0
FTL_0046	FTT1647c	diyroorotate dehydrogenase	*pyrD*	7.1E-05	-2.0
FTL_0345	FTT0849	bile acid symporter family protein		1.1E-03	-2.1
FTL_0680	FTT0563	polyamine transporter, subunit H, ABC transporter, membrane protein	*potH*	1.0E-03	-2.1
FTL_0075	FTT1674	riboflavin synthase beta subunit (6,7-dimethl-8-ribityllumazine	*ribH*	1.2E-06	-2.1

		synthase)			
FTL_0261	FTT0350	DNA-directed RNA polymerase, alpha subunit	*rpoA2*	1.8E-04	-2.1
FTL_0245	FTT0334	30S ribosomal protein S17	*rpsQ*	1.6E-03	-2.1
FTL_1185	FTT1275	macrophage growth locus, subunit A	*mglA*	4.2E-06	-2.1
FTL_1025	FTT1061c	30S ribosomal protein S18	*rpsR*	1.2E-03	-2.1
FTL_0679	FTT0564	polyamine transporter, subunit I, ABC transporter, membrane protein	*potI*	1.0E-02	-2.2
FTL_0045	FTT1648c	Orotidine 5'-phosphate decarboxylase	*pyrF*	1.6E-07	-2.2
FTL_1118	FTT1085	hypothetical protein		1.9E-05	-2.2
FTL_1868	FTT1727c	multidrug resistance protein, membrane located		2.4E-02	-2.2
FTL_0685	FTT1259	NH(3)-dependent NAD(+) synthetase	*nadE*	1.5E-06	-2.3
FTL_1190	FTT1270c	Chaperone protein grpE (heat shock protein family 70 cofactor)	*grpE*	3.6E-03	-2.3
FTL_0337	NA[b]	pseudogene		2.0E-08	-2.4
FTL_0843	FTT1120c	queuine tRNA-ribosyltransferase.	*tgt*	1.4E-05	-2.4
FTL_0863	FTT0598c	Sodium-dicarboxylate symporter family protein		5.3E-07	-3.0
FTL_1478	FTT1317c	Inosine-5-monophosphate dehydrogenase	*guaB*	1.3E-05	-3.1
FTL_0382	FTT0881c	amino acid permease		1.9E-08	-3.5

[a]The open reading frame (ORF) designations are adopted from the annotations of the genomes of the LVS (GenBank Genome Accession No. NC_007880) and Schu S4 strain (GenBank Genome Accession No. NC_006570). [b]NA denotes the absence of an ortholog in the indicated strain.

B. FslC is required for production of siderophores

The gene *fslC*, also annotated as *lysA*, encodes a putative diaminopimelate decarboxylase, which catalyzes the last step of L-lysine biosynthesis in *E. coli* (75). Since no complete L-lysine biosynthesis pathway is identifiable by bioinformatics in *F. tularensis*, the function of FslC in this organism remains unclear. To determine the biological function of FslC, the gene was inactivated by in-frame deletion. Failure of both the wild-type LVS and the Δ*fslC* mutant to grow in CDM deficient in L-lysine (data not shown) suggested that the *F. tularensis* LVS does not possess a pathway for biosynthesis of L-lysine.

FslA of *F. tularensis* has been shown to be involved in production of siderophores (39, 122). Since it is encoded by a gene in the same operon, FslC might have a similar biological function. Indeed, cultivation of bacteria on CAS plates showed that the wild-type LVS produced siderophores, but the Δ*fslC* mutant did not. Complementation by expression of *fslC* in *trans* restored the production of siderophores to the same level as in the wild-type LVS (Fig. 4A), whereas the empty vector did not rescue the phenotype (data not shown). Similar results were observed when liquid media conditioned by the wild-type LVS, the Δ*fslC* mutant, or the complemented Δ*fslC* bacteria were subjected to a CAS assay. Che-CDM conditioned by the Δ*fslC* mutant showed little siderophore activity, but both the wild-type LVS and the complemented Δ*fslC* strain produced high amounts of siderophores in Che-CDM with limited iron (180 nM or 360 nM). As would be expected for iron-regulated molecules, the levels of siderophores decreased in Che-CDM with a

high concentration (7.2 μM) of iron (Fig. 4B).

C. FeoB is also involved in iron acquisition

The Δ*fslC* mutant grew similarly to wild-type bacteria in MH+ (Fig. 5A). Since iron is an essential nutrient for *F. tularensis* (39, 122), this observation suggested that *F. tularensis* possesses pathways for acquisition of iron in addition to siderophores. A gene encoding a putative ferrous iron transporter, *feoB* (FTL_0133), was identified in the genome of the LVS. Inactivation of *feoB* of the LVS by insertion of a group II intron completely blocked the growth in AML12 hepatocytes and attenuated virulence in mice (data not shown). However, the phenotype of the mutant strain was not restored by a complementing plasmid. In addition, a *feoB*::Tn*5* transposon mutant of the LVS grew normally in AML12 cells. These results suggested that the altered phenotype of the group II intron mutant might not be specific to inactivation of *feoB*. Therefore, it was decided to make an in-frame deletion of the gene. In-frame deletion of *feoB* significantly slowed the growth of bacteria on Chocolate II agar, as shown by a substantially smaller size of colonies compared to the wild-type LVS. Supplementation of the agar with ferric pyrophosphate restored the normal replication of the Δ*feoB* mutant (Fig. 4C). However, supplementation did not alter growth of the wild-type LVS (data not shown), indicating that the small colony size of the Δ*feoB* mutant strain was due to its inability to acquire iron efficiently. Eleven attempts to generate *F. tularensis* lacking both *fslC* and *feoB* failed. This failure suggests that bacteria that lack the two genes are not viable and strongly implies that both FslC and FeoB are involved in acquisition of iron.

Figure 4. The Δ*fslC* mutant fails to produce siderophores, and the growth of the Δ*feoB* mutant is diminished on Chocolate II agar.
(A) Five µl of broth cultures containing the wild-type LVS, the Δ*fslC* mutant, or the complemented Δ*fslC* strain were spotted on CAS plates and incubated for 60 h. Production of siderophores is indicated by orange halos surrounding the bacteria. (B) The wild-type LVS, Δ*fslC* mutant, or complemented Δ*fslC* strain was inoculated into Che-CDM with indicated concentrations of iron. Siderophore activity in the conditioned media was measured after 120 h and normalized to the OD_{600}. (C) A broth culture of the Δ*feoB* mutant was plated onto Chocolate II agar or Chocolate II agar supplemented with ferric pyrophosphate and incubated for 48 h. The size of colonies was compared to that of the LVS organisms grown on unsupplemented agar.

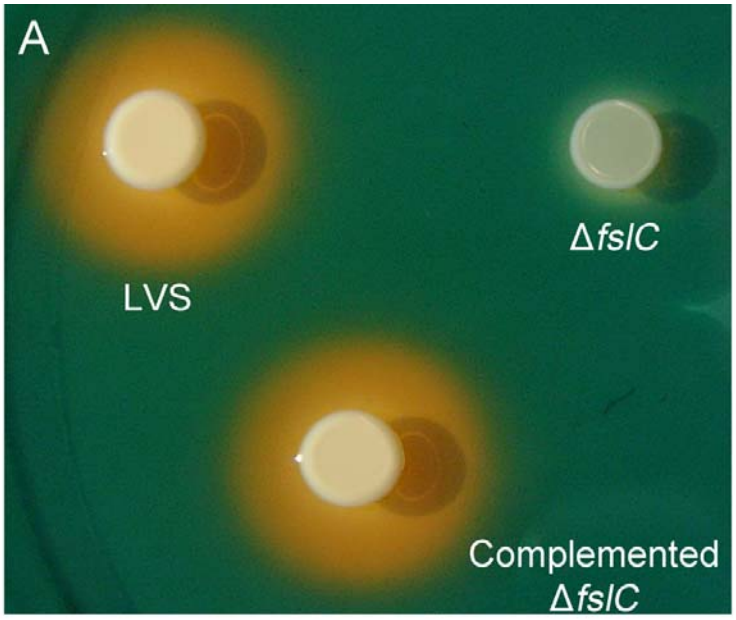
A
LVS
ΔfslC
Complemented
ΔfslC

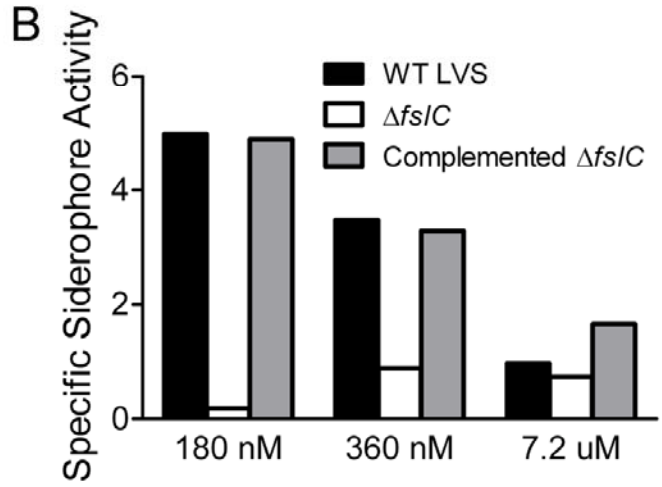
B
Specific Siderophore Activity
6
4
2
0
WT LVS
ΔfslC
Complemented ΔfslC
180 nM
360 nM
7.2 uM

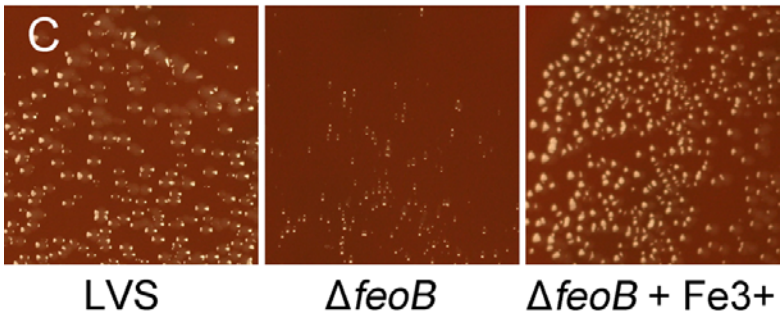
C
LVS
ΔfeoB
ΔfeoB + Fe3+

D. Growth of the Δ*fslC* and Δ*feoB* mutants is inhibited in iron-restricted broth

The wild-type LVS replicated equally well in either MH II broth supplemented with IsoVitalex and ferric pyrophosphate (MH+) or MH II broth containing only IsoVitalex (MH-). Like the Δ*fslC* mutant, the Δ*feoB* strain grew similarly to the wild-type LVS in either of these culture media, which are both relatively rich in iron (Fig. 5A and 5B). To create an environment in which iron was restricted, the ferric iron-specific chelator DFO was added to MH- to a final concentration of 90 μM (MH-/DFO). The growth of both mutants and the wild-type LVS was completely inhibited in MH-/DFO. Addition of 330 μM ferric iron pyrophosphate after 47 h of culture restored the ability of all strains to replicate (Fig. 5C). This result confirms that iron is an essential nutrient for the organism and demonstrates that the majority of iron in the MH- broth is ferric iron.

Although MH- broth is not supplemented with ferrous iron, this form of iron may be present in low amounts due to equilibration between Fe^{2+} and Fe^{3+}. Addition of the chelator DIP to MH- broth binds the ferrous iron, making it unavailable to the bacteria. Indeed, addition of DIP to MH- prolonged the pre-log phase of the growth curve for wild-type and mutant strains, compared to their replication in MH+ and MH- media. The growth of the Δ*feoB* mutant was only slightly inhibited compared to the wild-type LVS (Fig. 5D). The Δ*fslC* mutant was more sensitive to chelation of ferrous iron by DIP, and the complementing plasmid restored its growth to near-normal levels (Fig. 5E). The greater sensitivity of the Δ*fslC* mutant to DIP is consistent with the loss of the siderophore-ferric iron pathway in this strain, which should render it more dependent on

ferrous iron.

Che-CDM with defined concentrations of iron was used to further examine growth of the wild-type LVS, the Δ*fslC* mutant, and the Δ*feoB* strain in environments rich or poor in this nutrient. Although ferrous iron was added to the medium, oxidation will result in a mixture of the ferrous and ferric forms. The wild-type LVS, the Δ*fslC* mutant, the Δ*feoB* mutant, and the complemented strains grew similarly in Che-CDM replete with iron (7.2 μM), although growth of the complemented Δ*fslC* mutant lagged slightly at early time points (Fig. 6A). In the presence of 360 nM iron, the wild-type LVS grew to a lesser density than in the presence of 7.2 μM iron, and the OD_{600} declined at later time points. With 360 nM iron, the Δ*feoB* mutant began to grow only after a long lag phase, and replication of the Δ*fslC* mutant was nearly completely inhibited (Fig. 6B). Supplementation with 720 nM iron better supported the growth of all strains. It greatly shortened the pre-log phase for the Δ*feoB* mutant and permitted growth of the Δ*fslC* mutant after a long lag phase (Fig. 6C). However, growth of the Δ*fslC* strain under iron-restricted conditions was not restored by complementation, and in fact the complemented strain grew more poorly than the mutant itself (Fig. 6B and 6C). This observation suggests that the presence of the complementing plasmid may be deleterious under some conditions. Nevertheless, as mentioned, the complemented Δ*fslC* strain produced wild-type levels of siderophores (Fig. 4A and 4B) and grew comparably to wild-type bacteria in MH-/DIP broth (Fig. 5E).

Similarly, the growth of the Δ*feoB* strain in medium with restricted iron was not

rescued by complementation (Fig. 6B and 6C). To gain further evidence that the phenotype of this strain was specific to deletion of *feoB*, we also examined the transposon mutant *feoB*::Tn*5* (120). In Che-CDM replete with iron (7.2 μM), the Δ*feoB* and *feoB*::Tn*5* strains grew as well as the wild-type LVS (Fig. 7A). The conditioned media were subjected to CAS assays, which showed that the mutants and the wild-type LVS produced similar levels of siderophores in medium with this concentration of iron (Fig. 7B). In Che-CDM with restricted iron (360 nM), growth of the mutants lagged compared to the wild-type LVS at early times, but ultimately caught up (Fig. 7C). CAS assays demonstrated that production of siderophores by the mutants was slower compared to the wild-type LVS and that their accumulation correlated with the onset of rapid growth in this medium (Fig. 7D). These results suggest that FeoB supports growth of the bacteria before adequate levels of siderophores accumulate.

Figure 5. The growth of *F. tularensis* is inhibited in MH II broth with limited availability of iron.
Growth of the wild-type LVS, Δ*fslC* mutant, Δ*feoB* mutant, or complemented strains was assessed in (A) MH II broth supplemented with ferric pyrophosphate (designated MH+); (B) MH II broth without addition of ferric pyrophosphate (MH-); (C) MH- containing the ferric iron chelator DFO; or (D and E) MH- containing the ferrous iron chelator DIP. Growth was determined by measuring the OD_{600} of the cultures. In Panel C, replication of the bacteria was stimulated by addition of ferric iron at 47 h (indicated by the plus sign). This study was repeated two more times, yielding similar results.

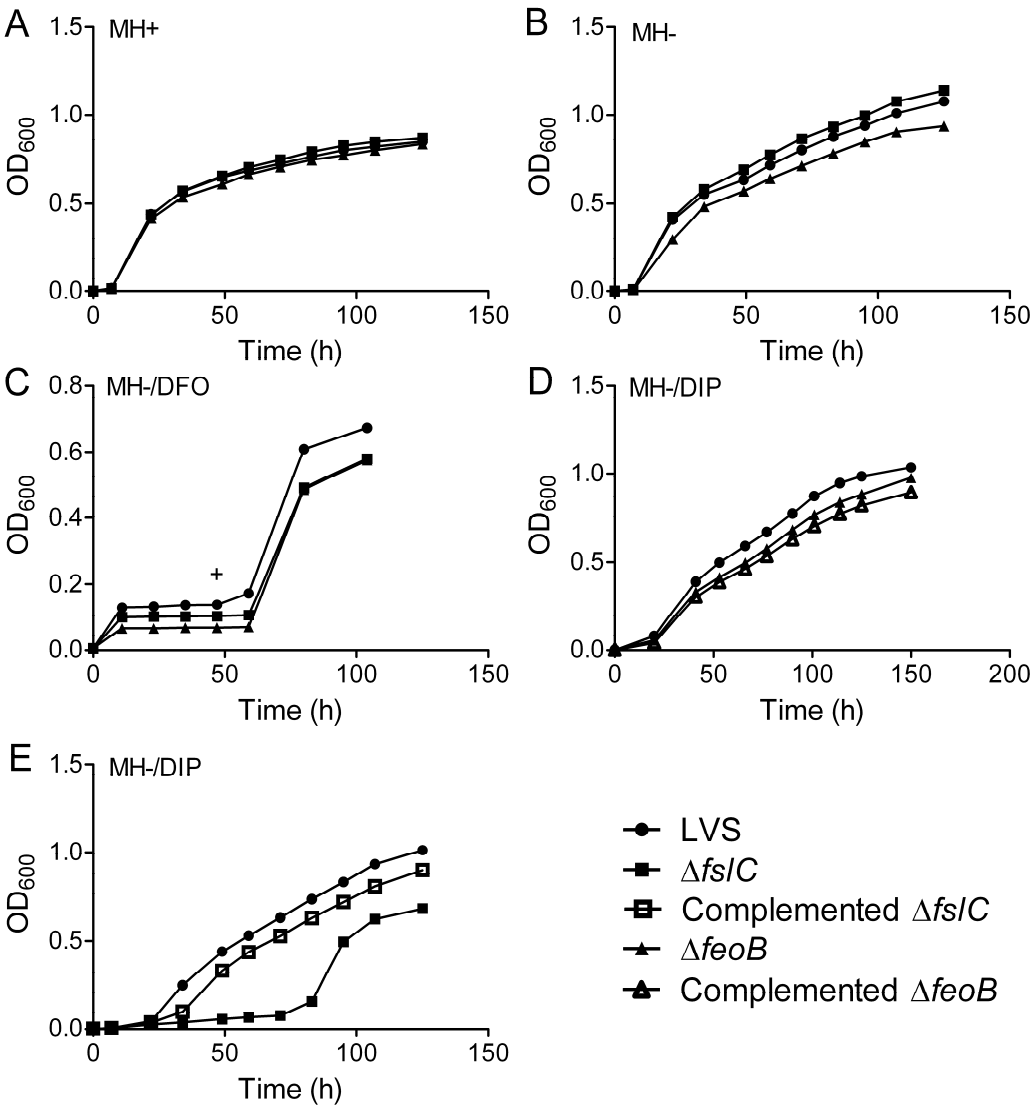
A
MH+
B
MH-
C
MH-/DFO
D
MH-/DIP
E
MH-/DIP
OD600
Time (h)
LVS
ΔfslC
Complemented ΔfslC
ΔfeoB
Complemented ΔfeoB

Figure 6. The Δ*fslC* and Δ*feoB* mutants show impaired growth in defined media containing low levels of iron.
The wild-type LVS, Δ*fslC* mutant, Δ*feoB* mutant, or complemented strains were inoculated into Che-CDM containing iron at a concentration of (A) 7.2 μM, (B) 360 nM, or (C) 720 nM. Growth was assessed by measuring the OD_{600}. This experiment was repeated two more times with similar results

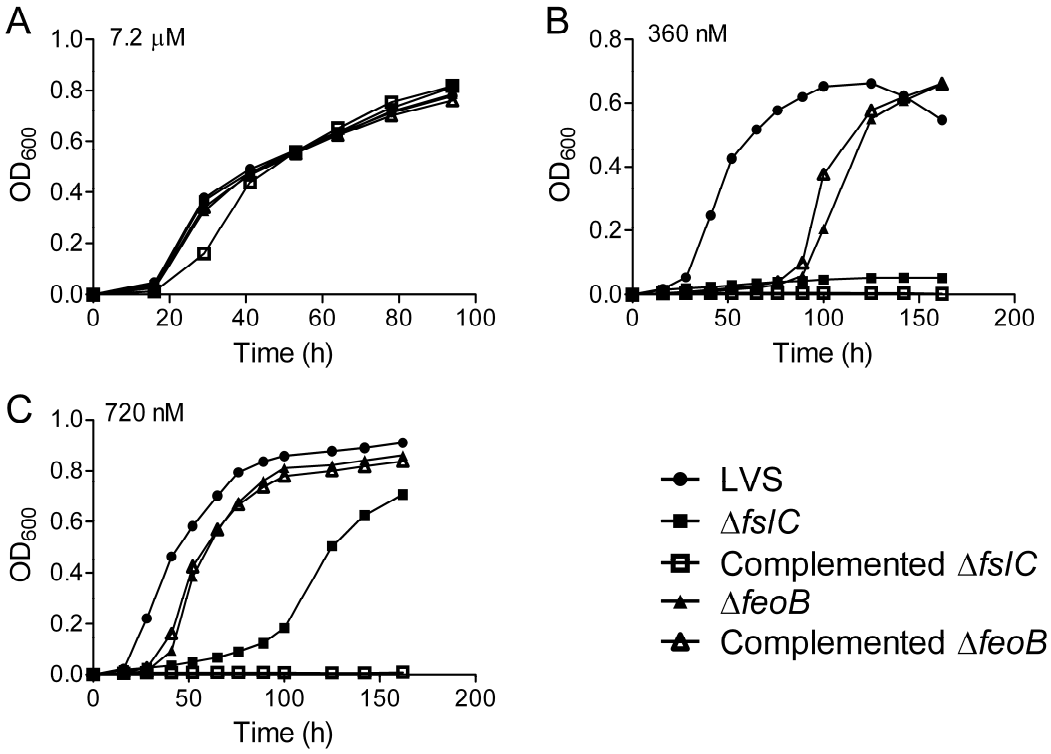
A
7.2 μM
OD600
Time (h)
B
360 nM
OD600
Time (h)
C
720 nM
OD600
Time (h)
LVS
ΔfslC
Complemented ΔfslC
ΔfeoB
Complemented ΔfeoB

Figure 7. Production of siderophores by *F. tularensis* lacking FeoB is delayed in iron-restricted media.
The wild-type LVS, Δ*feoB* mutant, or *feoB*::Tn*5* strain was inoculated into Che-CDM containing (A and B) 7.2 μM or (C and D) 360 nM iron. At indicated times, the OD_{600} of each culture was measured (A and C), and the siderophore activity (B and D) in the conditioned media was assayed. Data represent one experiment, which was repeated with similar results.

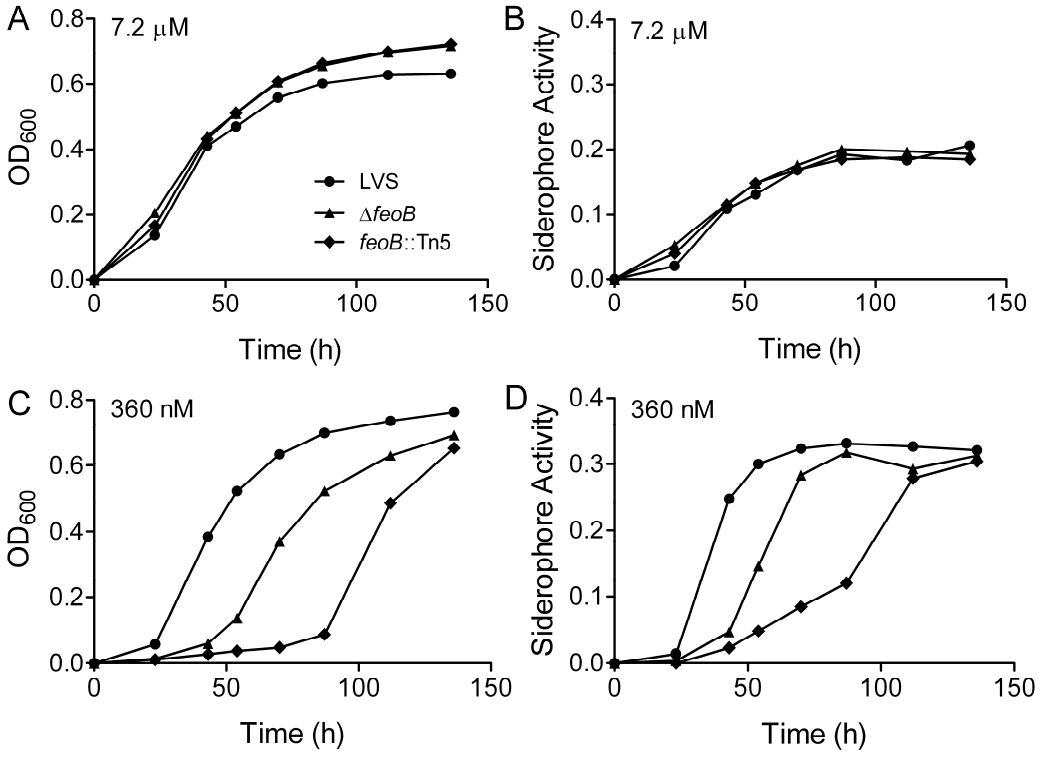
A
7.2 μM
OD600
0.8
0.6
0.4
0.2
0.0
0
50
100
150
Time (h)
LVS
ΔfeoB
feoB::Tn5
B
7.2 μM
Siderophore Activity
0.4
0.3
0.2
0.1
0.0
0
50
100
150
Time (h)
C
360 nM
OD600
0.8
0.6
0.4
0.2
0.0
0
50
100
150
Time (h)
D
360 nM
Siderophore Activity
0.4
0.3
0.2
0.1
0.0
0
50
100
150
Time (h)

E. Loss of FslC or FeoB affects growth of *F. tularensis* in hepatocytes

To address whether FslC and FeoB are important for intracellular growth, murine FL83B hepatocytic cells were incubated with the wild-type LVS or the Δ*fslC*, Δ*feoB*, or *feoB*::Tn*5* mutants at a MOI of 1,000 for 2 h. Hepatocytes were washed and incubated with gentamicin for additional 1 h or 22 h. The amounts of viable intracellular bacteria were determined by CFU assays, and the extent of intracellular growth was determined by calculating the fold changes between 3 and 24 h after infection was initiated. Intracellular growth of the Δ*fslC* mutant (1500-fold) was similar to that of the wild-type LVS (1680-fold), but intracellular replication of the Δ*feoB* mutant (110-fold) and the *feoB*::Tn*5* mutant (40-fold) was greatly reduced (Fig. 8). Complementation of the Δ*feoB* mutant did not restore its ability to grow.

In contrast, the Δ*fslC* and Δ*feoB* mutants grew similarly to the wild-type LVS in AML12 hepatocytic cells (Table 3). We reasoned that AML12 cells might contain a higher level of iron than do FL83B cells, thus allowing even the mutant strains to replicate well. To test this premise, the chelator DIP was used to scavenge intracellular ferrous iron (95, 96). When the AML12 cells were treated with 75 μM DIP for 24 h prior to infection, the uptake of the different strains at 3 h post-infection was the same (data not shown). However, the number of intracellular Δ*fslC* and Δ*feoB* organisms at 24 h post-infection was about half the number of wild-type bacteria (Table 3). As for AML12 cells, human macrophages supported the replication of the Δ*fslC*, the Δ*feoB*, and the wild-type strains to similar levels (data not shown).

Table 3: Growth of *F. tularensis* Δ*fslC* and Δ*feoB* mutants in AML12 hepatocytic cells is inhibited by the ferrous iron chelator DIP[a]

Strain	Control (CFU×10^4)	% of Control LVS	DIP (CFU×10^4)	% of DIP-treated LVS
LVS	775 ± 39	100	211 ± 43	100
Δ*fslC*	653 ± 125	84	114 ± 19[b]	54
Δ*feoB*	861 ± 60	111	102 ± 15[b]	48
Complemented Δ*fslC*	704 ± 133	91	111 ± 9[b]	52
Complemented Δ*feoB*	979 ± 129	126	90 ± 22[b]	42

[a]Replication was measured by CFU assay in AML12 cells pre-treated with DIP or left untreated (control). [b]Significantly different ($P < 0.001$) from the DIP-treated LVS group.

Figure 8. Growth of the Δ*feoB* mutant is diminished in FL83B hepatocytic cells. FL83B cells were incubated with the indicated strains for 2 h. Extracellular bacteria were removed, cells were incubated with gentamicin for an additional 1 h or 22 h, and the viable intracellular bacteria were enumerated by CFU assays. Because levels of uptake of the various strains differed at 3 h, data are depicted as fold-changes from 3 h to 24 h post-infection. Bars represent the means ± SD of four replicate samples. **P* < 0.001 compared to the LVS. This experiment was repeated once more with similar results.

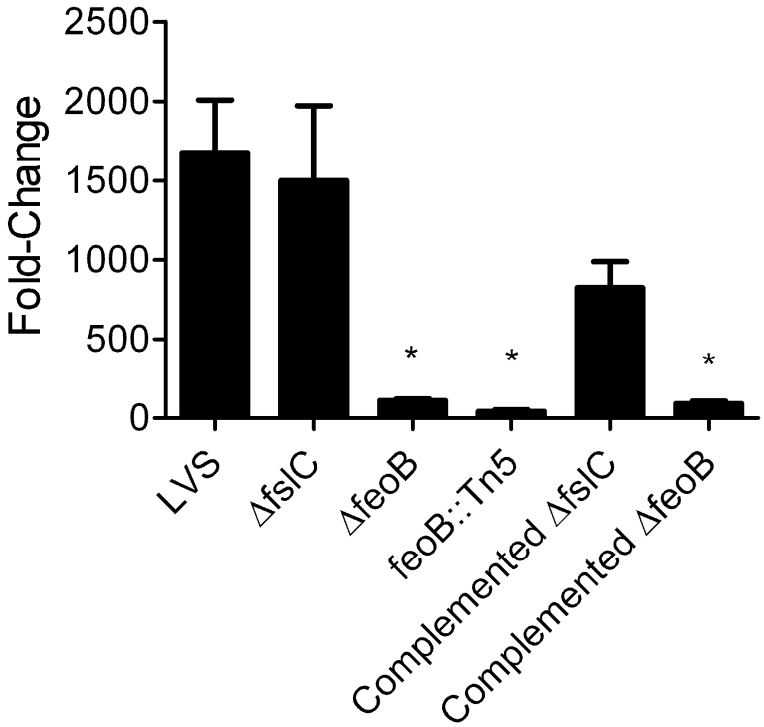
Fold-Change
2500
2000
1500
1000
500
0
*
*
*
LVS
ΔfslC
ΔfeoB
feoB::Tn5
Complemented ΔfslC
Complemented ΔfeoB

F. Loss of FslC or FeoB diminishes the virulence of *F. tularensis* in mice

To compare the virulence of the wild-type LVS with that of the mutant and complemented strains, 5×10^5 bacteria were administered to C3H/HeN mice intranasally. All of the mice infected with the LVS displayed severe signs of disease, and most died within 2 weeks after infection (Fig. 9A and 9B). The mice infected with the Δ*fslC* (Fig. 9A) and Δ*feoB* (Fig. 9B) strains became sick, but the virulence of both mutants was significantly reduced. In neither case did complementation restore virulence. However, the *feoB*::Tn*5* mutant, like the Δ*feoB* strain, was significantly attenuated (Fig. 9B). Therefore, it appears that disruption of pathways for acquisition of iron impairs the ability of *F. tularensis* to cause disease.

Figure 9. Loss of FslC or FeoB reduces the virulence of *F. tularensis* in mice.
C3H/HeN mice were inoculated with 5×10^5 organisms of the indicated strains and monitored for survival. Results for the Δ*fslC* mutant and its complemented strain are shown in Panel A; data for the Δ*feoB* mutant, its complemented strain, and the *feoB*::Tn*5* mutant are depicted in Panel B. Each panel contains data collected from two independent experiments. Compared to that of the LVS, the virulence of the Δ*fslC* ($P = 0.02$), Δ*feoB* ($P = 0.02$), and *feoB*::Tn*5* ($P < 0.001$) mutants was significantly reduced.

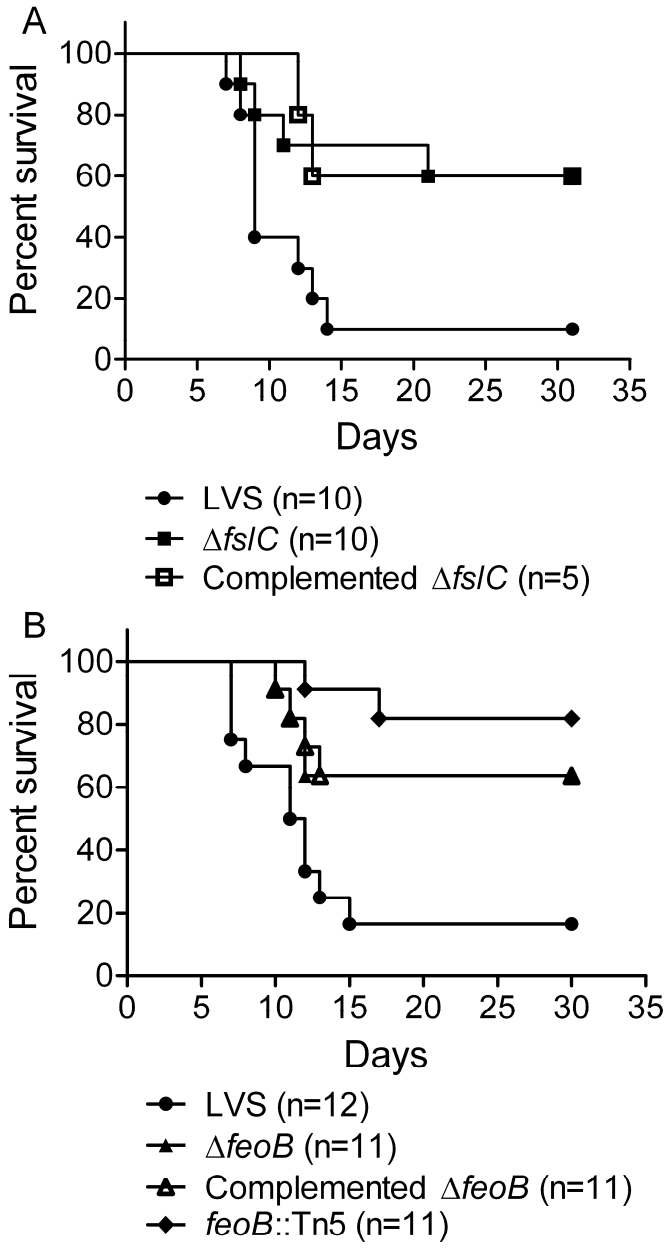
A
Percent survival
100
80
60
40
20
0
0 5 10 15 20 25 30 35
Days
LVS (n=10)
ΔfslC (n=10)
Complemented ΔfslC (n=5)
B
Percent survival
100
80
60
40
20
0
0 5 10 15 20 25 30 35
Days
LVS (n=12)
ΔfeoB (n=11)
Complemented ΔfeoB (n=11)
feoB::Tn5 (n=11)

III. Response of hepatocytes to infection with the LVS

A. Infection with the LVS eventually causes death of hepatocytes

Unless they are cleared by immune cells, hepatocytes *in vivo* appear to tolerate infection with the *F. tularensis* LVS rather well (31, 103). To determine the final fate of infected hepatocytes *in vitro*, LDH activity in conditioned media was assayed. LDH is an intracellular enzyme that is released when cells die and subsequently lyse. Murine FL83B or AML12 cells were infected with the LVS for 24 h. The extracellular bacteria then were removed, and the cells were incubated in fresh medium with gentamicin for an additional 24 h or 48 h. As determined by release of LDH, both FL83B and AML12 cells tolerated infection with the LVS well for the first 48 h of infection, but extensive death was observed after 72 h of infection (Table 4).

Table 4: The *F. tularensis* LVS kills hepatocytes after an extended period of infection[a]

Cell line	LDH release (% of total)	
	48 h post-infection	72 h post-infection
FL83B cells (Experiment 1)	6.8	67.5
FL83B cells (Experiment 2)	5.2	46.9
AML12 cells (Experiment 1)	0	23.6

[a] Hepatocytes were infected with the LVS at a MOI of 150 for 24 h. Release of LDH (expressed as a percentage of the total content in the hepatocytes) was measured after an additional 24 h or 48 h of incubation.

B. The transcriptional profile of AML12 cells infected with the LVS is different from that of uninfected cells

To assess how AML12 cells respond to infection with the LVS, cDNA microarray analysis was performed to compare the global gene expression of infected hepatocytes with that of uninfected cells. AML12 cells were infected with the LVS at an initial MOI of 10,000 for 2 h or an initial MOI of 1,000 for 6 h, 12 h, or 24 h. The total RNA of infected or uninfected cells then was isolated and processed for microarray analysis. Gene expression was extensively altered 2 h after infection, with about 250 genes up-regulated more than 2-fold. The most highly up-regulated genes included a number that encode proinflammatory cytokines, such as *Csf2*, *Cxcl2*, *Csf3*, *Ccl20*, and *Tnf*. The number of genes up-regulated more than 2-fold increased to 700 after 6 h of infection, and the fold-change of each gene typically was higher than at 2 h of infection. The amount of up-regulated genes and the fold-changes in expression declined thereafter. The most highly up-regulated genes at 6 h post-infection included *Csf3*, *Cxcl2*, *Csf2*, *Ccl20*, *Saa3*, *Cxcl1*, *Tlr2*, *Cxcl5*, *Icam1*, *Csf1*, *Cxcl16*, and *Ccl7* (Table 5). At 6 h post-infection, up-regulated expression of *Csf3*, *Cxcl2*, *Icam1*, and *Nos2* was verified by real-time RT-PCR with fold-changes of 1900, 470, 15, and 4200, respectively.

Microarray analysis of FL83B hepatocytes also was carried out at 2 h and 12 h after infection with the LVS. The global gene expression profile of infected FL83B cells was different from that of infected AML12 cells. Overall, the fold-changes of gene expression were much lower than those in AML12 cells (data not shown). Several genes

were up-regulated in both FL83B and AML12 cells, such as *Saa3*, *Nos2*, *Ccl20*, and *Cxcl1*. However, many genes that were increased after infection in AML12 cells were not up-regulated in the FL83B line. These results indicate that different lines of murine hepatocytic cells respond to infection with the LVS in different manners.

Table 5: Selected up-regulated genes of AML12 cells infected with the LVS[a]

Oligo ID	Gene	Fold-Changes			
		2h	6h	12h	24h
mMA035260	*Csf3*	31.2	103.2	52.9	3.0
mMC002554	*Csf3*	28.5	97.4	34.5	2.8
mMC022593	*Cxcl2*	35.0	48.1	35.4	5.1
mMC014357	*Csf2*	50.5	37.2	19.2	1.6
mMC015165	*Nos2*	1.7	24.2	3.1	1.4
mMC018537	*Ccl20*	22.1	20.8	20.4	4.4
mMC007240	*Saa3*	8.0	18.2	17.9	6.3
mMC009367	*Atf3*	3.9	18.1	14.3	7.2
mMA035116	*Pfkfb3*	4.7	15.2	5.9	2.5
mMC001897	*Pgf*	3.0	15.1	9.2	6.1
mMC023634	*Cxcl1*	5.4	13.7	19.8	2.4
mMC012626	*Tlr2*	5.2	13.0	3.9	1.1
mMC023098	*Pde4b*	4.4	12.1	3.8	1.1
mMC012724	*Fosl2*	2.5	11.8	8.6	2.8
mMC014914	*Cxcl5*	5.4	11.7	4.8	2.0
mMC020025	*Fosl2*	2.4	11.6	9.5	2.5
mMC017562	*Ripk2*	5.2	11.2	3.0	-1.1
mMC012010	*Icam1*	7.3	11.2	8.0	1.5
mMC019165	*E130306I01Rik*	7.2	10.4	7.7	1.7
mMC011682	*Tnfaip2*	7.4	9.8	6.5	1.4
mMC002655	*Nfkbiz*	10.9	9.6	6.5	2.0
mMC002384	*Gadd45b*	5.1	9.0	9.7	5.3
mMC024723	*Pfkfb3*	3.4	8.7	4.4	2.2
mMC009470	*Rgs16*	4.0	8.5	1.7	1.1
mMA032453	*Irf1*	7.9	8.5	6.7	2.1
mMC020606	*Irf1*	7.0	8.5	7.7	1.8
mMA033880	*CSF-1*	2.4	8.4	13.3	2.8
mMA034482	*Tnfaip2*	5.9	8.2	6.6	1.4
mMC012174	*Cxcl16*	3.0	8.1	6.0	-1.2
mMC005764	*Ccl7*	3.4	8.0	14.1	3.1
mMC002633	*Tnfaip3*	5.8	7.8	6.8	2.4
mMR029909	*Ptges*	1.7	7.7	7.3	1.3
mMA032268	*Irf1*	9.9	7.4	6.6	2.0
mMC012863	*Myd116*	3.1	7.2	8.0	8.4
mMR029910	*Ero1l*	1.1	7.2	8.8	8.2
mMC006715	*Adm*	1.9	7.1	6.0	3.8

mMC021520	*9430076C15Rik*	-1.0	7.0	5.2	2.9
mMC024156	*Ccrl2*	3.9	6.9	2.0	1.6
mMC019780	*Cd44*	2.5	6.8	9.9	1.6
mMC011325	*8430408G22Rik*	7.6	6.8	5.0	1.6
mMC009923	*Hmox1*	1.3	6.7	9.4	5.1
mMR001166	*Cxcl16*	2.4	6.7	5.9	1.7
mMR028290	*Mad*	1.2	6.6	8.0	2.2
mMC025031	*Eno2*	1.4	6.4	5.1	3.9
mMC016605	*Tnf*	18.5	6.4	2.0	1.2
mMC023498	*Elf3*	7.3	6.3	3.2	1.9
mMC022571	*Saa1*	2.3	6.1	2.3	1.3
mMC021996	*Saa2*	2.1	5.9	2.5	-1.4
mMC012054	*Ier3*	2.5	5.9	9.3	3.4
mMC012597	*Nfkbia*	6.6	5.9	7.7	3.0
mMC008044	*Cilp2*	5.6	5.8	1.8	-1.1
mMC014819	*Lcn2*	1.8	5.8	5.1	6.7
mMC003881	*Nr1d1*	1.6	5.8	3.8	5.7
mMA031311	*Nos2*	1.7	5.8	3.0	1.4
mMC019577	*Pdcd1lg1*	1.8	5.7	4.2	1.3
mMC002484	*Irg1*	1.8	5.7	2.1	1.3
mMC003495	*Gbp4*	1.5	5.6	2.1	1.4
mMC004291	*Elf3*	8.5	5.5	3.4	2.7
mMC022886	*Zfp36*	6.4	5.3	3.4	1.1
mMA034934	*Tnfrsf6*	2.2	5.2	2.3	2.0
mMC021481	*Ptges*	1.3	5.2	3.6	1.3
mMC021021	*Egln3*	2.5	5.1	2.2	1.4
mMC017365	*Ndrg1*	1.6	5.1	2.2	2.7
mMA032465	*Itgb6*	4.5	5.1	2.5	1.0
mMR028298	*H2-D1*	3.2	5.1	2.4	1.4
mMA033236	*BC032266*	1.4	5.1	1.9	1.1
mMC001582	*Mmp13*	1.8	5.1	2.1	1.1
mMC017911	*Sca1*	-1.1	5.1	2.0	1.4
mMR030566	*Vcam1*	4.7	5.0	1.4	-3.7
mMC009625	*St5*	1.4	5.0	1.9	-1.1

[a] Genes upregulated more than 5-fold at 6 h of infection are listed here. Fold-changes of the same gene at 2 h, 12 h, and 24 h of infection are also shown in the table.

C. Hepatocytes infected with the LVS produce cytokines and chemokines

Since expression of some cytokines and chemokines in AML12 cells was up-regulated at the transcriptional level as demonstrated by microarray analysis and real-time RT-PCR, production of the corresponding proteins was determined by ELISA. AML12 cells were infected with the LVS at an initial MOI of 1,000 or treated with a sham preparation of bacteria for 4 h or 24 h. Conditioned media of uninfected, infected, and sham-treated cells were collected for analysis. The uninfected and sham-treated AML12 cells produced no detectable CXCL2, while cells infected with the LVS for 4 h produced more than 100 pg/ml of CXCL2. After 24 h of infection, the concentration of this chemokine increased to 300 pg/ml (Fig. 10A). Similarly, uninfected and sham-treated AML12 cells did not produce CSF3. Production of CSF3 was not detectable after 4 h of infection, but the concentration reached over 200 pg/ml at 24 h post-infection (Fig. 10B). Constitutive production of CCL20 was observed in control AML12 cells. However, infection with the LVS significantly boosted secretion of this chemokine (Fig. 10C). AML12 cells infected with the LVS did not produce CCL5 (RANTES) during the first 24 h of infection, and only a low amount of CCL5 was secreted over the next 24 h. However, treatment with IFN-γ induced production of CCL5 by the AML12 cells, showing that this line is capable of making CCL5 when stimulated appropriately (Fig. 10D).

Figure 10. AML12 cells infected with the LVS produce cytokines and chemokines. To assay secretion of (A) CXCL2, (B) CSF3, or (C) CCL20, AML12 cells were infected with the LVS at a MOI of 1,000 for 4 h or 24 h. To test the production of CCL5, AML12 cells were infected with the LVS for 24 h and incubated in fresh medium for an additional 24 h. Treatment with 100 ng/ml of IFN-γ was used as positive control (D). The conditioned media of uninfected cells, sham-treated cells, and infected cells were collected for analysis by ELISA. Bars represent the means ± SD of three samples. **, $P < 0.01$; ***, $P < 0.001$. These experiments were repeated two more times with similar results.

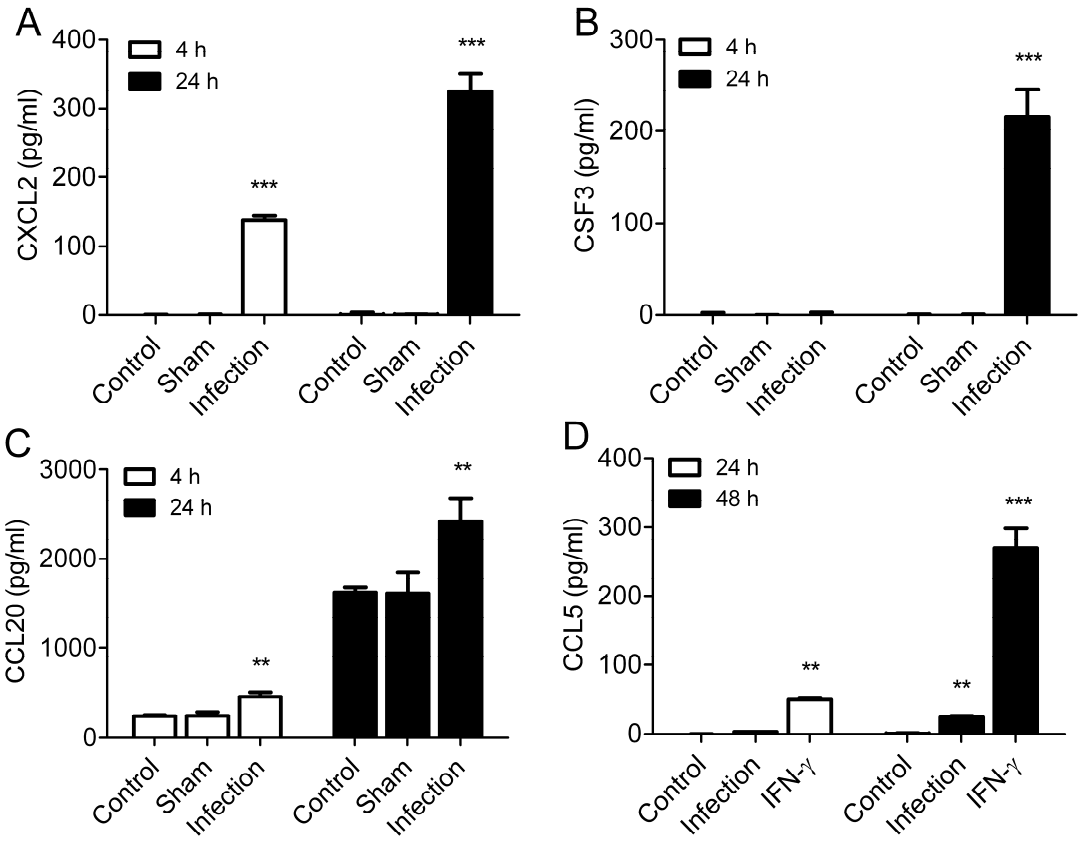
A
CXCL2 (pg/ml)
400
300
200
100
0
4 h
24 h
***
***
Control
Sham
Infection
Control
Sham
Infection
B
CSF3 (pg/ml)
300
200
100
0
4 h
24 h
***
Control
Sham
Infection
Control
Sham
Infection
C
CCL20 (pg/ml)
3000
2000
1000
0
4 h
24 h
**
**
Control
Sham
Infection
Control
Sham
Infection
D
CCL5 (pg/ml)
400
300
200
100
0
24 h
48 h
**
**
***
Control
Infection
IFN-γ
Control
Infection
IFN-γ

D. Hepatocytes infected with the LVS do not produce nitric oxide

Nitric oxide is an important mediator for inducing death of host cells and controlling the growth of intracellular bacteria in the livers of tularemic mice (14). Expression of *Nos2* was highly up-regulated in AML12 cells infected with the LVS for 6 h (Table 5). The gene *Nos2* encodes inducible nitric oxide synthase, which catalyzes the production of nitric oxide. However, even though expression of *Nos2* was up-regulated, nitric oxide was not detected in the conditioned medium of infected AML12 cells (data not shown). In agreement with this finding, treatment of AML12 cells with the nitric oxide synthase inhibitor L-NMMA did not influence the intracellular growth of the LVS (Fig. 11). These results indicate that nitric oxide is not utilized by hepatocytes to control the replication of the LVS.

E. Treatment of hepatocytes with IFN-γ inhibits intracellular growth of *F. tularensis*

Treatment of hepatocytes with IFN-γ inhibits intracellular growth of *Listeria monocytogenes* and *Legionella pneumophila* (21, 53, 56, 123), and IFN-γ is also important for controlling the progression of tularemia in the liver (14, 134). Therefore, the effect of IFN-γ on the growth of *F. tularensis* in hepatocytes was assessed *in vitro*. FL83B hepatocytic cells were treated with IFN-γ 24 h prior to infection with the LVS, simultaneously upon infection, or 24 h after infection was initiated. The cells were then incubated for an additional 24 h in the continued presence of IFN-γ, and the amount of viable intracellular bacteria was determined by CFU assay. Under all protocols, treatment of hepatocytes with IFN-γ significantly inhibited the intracellular replication of the LVS.

The effectiveness of IFN-γ depended on when it was added: the earlier the treatment began, the smaller the amount of viable intracellular bacteria recovered (Fig. 12).

Figure 11. Nitric oxide is not utilized to inhibit intracellular growth of the LVS. Cells were infected with the LVS at a MOI of 1,000 for 2 h. The extracellular bacteria were removed and the cells were incubated in fresh medium with gentamicin for the indicated times. The cultures were treated with the nitric oxide synthase inhibitor L-NMMA throughout the course of the experiment. At each time point, the intracellular bacteria were released by saponin, and the amount was determined by CFU assay. Data points represent the means ± SD of three replicate samples.

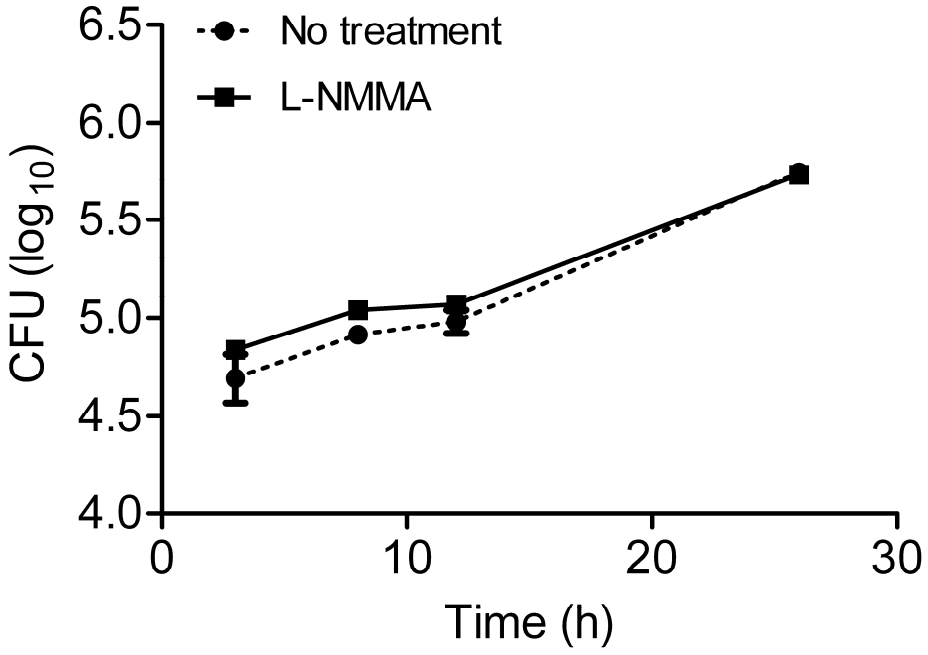
No treatment
L-NMMA
6.5
6.0
5.5
5.0
4.5
4.0
CFU (log10)
0
10
20
30
Time (h)

Figure 12. IFN-γ inhibits the growth of the LVS in AML12 hepatocytes.
AML12 cells were treated with 100 ng/ml of IFN-γ beginning 24 h prior to infection, at the same time as infection, or 24 h after initiation of infection. The IFN-γ-treated and untreated control cells were infected with the LVS for 24 h at an initial MOI of 1,000. The extracellular bacteria were removed, and the cells were incubated with IFN-γ and gentamicin for an additional 24 h. Intracellular bacteria were released by saponin, and the amount of viable bacteria was determined by CFU assay. Bars represent means ± SD of three replicate samples. **, $P < 0.01$; ***, $P < 0.001$.

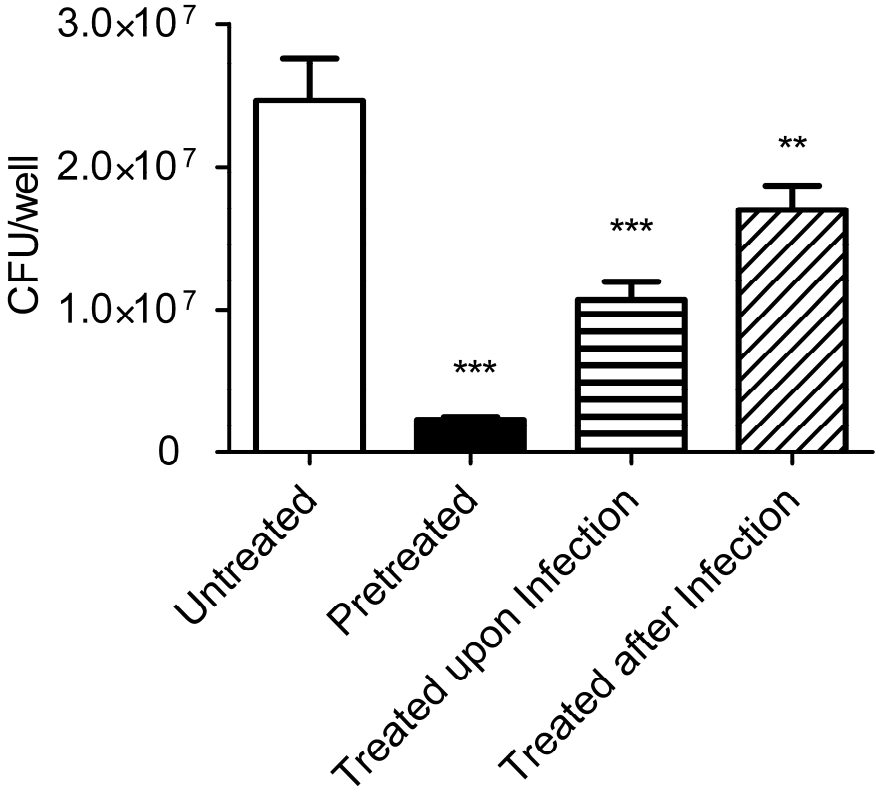
3.0×10^7
2.0×10^7
1.0×10^7
0
CFU/well
***
***
**
Untreated
Pretreated
Treated upon Infection
Treated after Infection

DISCUSSION

I. Pathways for acquisition of iron

In this study, I demonstrated that hepatocytic cells generally support extensive intracellular growth of the *F. tularensis* LVS and analyzed the gene expression of the bacteria within hepatocytes using cDNA microarrays. Four genes of the *fsl* operon were the most highly up-regulated. The *fsl* operon is involved in production of siderophore, which is used to take up ferric iron. Thus, up-regulation of these genes indicates restriction of iron in hepatocytes compared to MH II broth. Similar to our findings, expression of genes of the *fsl* operon is also increased when the Schu S4 strain grows in murine bone marrow-derived macrophages (132). Our data also showed that expression of genes of the *Francisella* pathogenicity island, which are required for replication in macrophages, was up-regulated. Expression of genes related to the general stress response and the oxidative stress response was not altered when the LVS grew in hepatocytes. However, these genes are generally up-regulated when the type A Schu S4 strain grows in bone marrow-derived macrophages (132).

Deletion of *fslC* eliminated production of siderophores and attenuated virulence in mice. However, the Δ*fslC* strain grew similarly to the wild-type LVS in hepatocytes, human monocyte-derived macrophages, and MH II broth, strongly suggesting that the LVS possesses other pathways for acquisition of iron. Our results show that FeoB, a putative ferrous iron transporter, is such an alternative pathway. Deletion of *feoB* reduced growth of the LVS in medium where iron was limited, markedly diminished replication in

FL83B hepatocytic cells, and attenuated virulence in mice.

The role of the *fsl* operon in acquisition of iron by *Francisella* has been investigated previously (39, 122). In *F. novicida* U112, the genes *fslA*, *fslB*, and *fslC* are all required for production of siderophores (60). In agreement, our data show that the FslC protein of the *F. tularensis* LVS is also necessary for secretion of siderophores. However, the growth of the LVS Δ*fslC* strain was similar to that of wild-type bacteria in broth containing abundant iron, suggesting that the LVS has other mechanisms to obtain iron. The Feo transport system is used by many other bacteria for acquisition of ferrous iron. Of 250 completely sequenced bacterial genomes, 46% possess genes of the Feo system (24). Mutation of *feo* genes in *E. coli* results in defective import of ferrous iron, lower levels of intracellular iron, and impaired ability to colonize the mouse intestine (63, 119). The structure of the transmembrane domain of FeoB and the mechanism by which this protein transports iron are unknown. Genes encoding FeoA and FeoB were identified in the LVS (122), but their biological functions had not been determined. Therefore, to determine definitively whether *feoB* is a potential pathway for acquisition of iron, in-frame deletion of the gene was performed.

Characterization of the Δ*feoB* and Δ*fslC* mutants demonstrated that both of the encoded proteins contribute to utilization of iron by *F. tularensis*. Similar growth of the wild-type LVS, the Δ*fslC* mutant, and the Δ*feoB* mutant in media replete with iron (Fig. 5A and 6A) revealed that neither the Fsl nor FeoB pathway by itself is essential for acquisition of iron. Loss of FeoB, however, resulted in retarded growth in defined

medium containing limited iron (Fig. 6B). Moreover, growth of the Δ*fslC* mutant in MH II broth was inhibited when ferrous iron was chelated (Fig. 5E), suggesting that the ferrous iron pathway becomes important when siderophores are absent. Nonetheless, our data indicate that the siderophore-ferric iron pathway provides *F. tularensis* with the bulk of this nutrient, at least when the organism is cultured in broth. Chelation of ferric iron almost completely inhibited growth of the LVS in MH II broth (Fig. 5C). Although replication of the Δ*feoB* and *feoB*::Tn*5* mutants was greatly delayed when iron was limited, a burst of growth occurred eventually, and the density of the cultures ultimately reached that of the wild-type LVS (Fig. 6B and 7C). This burst correlated with an increase in siderophore activity in the medium (Fig. 7D). It appears, then, that the Fsl pathway predominates under these conditions.

Our data showed that hepatocytic cell lines of murine and human origin generally supported the intracellular growth of the LVS. The mechanisms by which hepatocytes foster replication of *F. tularensis* are not known. However, abundant iron is likely available, since hepatocytes, along with erythrocytes, are the main host cells in which iron is stored (6). Our results and those of others indicate that the siderophore-ferric iron pathway is not essential for *F. tularensis* to acquire this intracellular iron. Growth of a Δ*fslA* mutant of the LVS in murine J774 macrophage-like cells is the same as that of the wild-type parental bacteria (39). Similarly, growth of our Δ*fslC* mutant in hepatocytic cells was equal to that of the wild-type LVS (Fig. 8). To avoid toxicity of free iron, its levels in hosts are tightly regulated. Extracellular iron is bound to proteins in the ferric

form. Free ferrous iron is needed for various physiological and pathological processes within host cells, but any excess is oxidized and either exported or stored bound to ferritin (41). Our data suggest that intracellular *F. tularensis* can acquire this ferrous iron via FeoB, since replication of the Δ*feoB* mutant was greatly reduced in FL83B hepatocytic cells (Fig. 8). In summary, it appears that *F. tularensis* relies mainly on the siderophore-ferric iron pathway to obtain iron from broth, but FeoB plays the predominant role within host cells. Notably, replication of the Δ*feoB* mutant was similar to that of the wild-type LVS in AML12 hepatocytic cells and human monocyte-derived macrophages. However, when AML12 cells were treated with a chelator to artificially limit their content of ferrous iron, intracellular replication of both the Δ*fslC* and Δ*feoB* strains was reduced by half (Table 1). This result suggests that levels of iron differ in various types of cells and that loss of either FslC or FeoB impairs the ability of intracellular *F. tularensis* to acquire iron when amounts are very limited.

Both FslC and FeoB contribute to the virulence of the LVS in mice. Our study showed that fewer mice infected intranasally with the Δ*fslC* mutant died compared to animals infected with the wild-type LVS (Fig. 9A). However, loss of FslA does not affect the virulence of *F. tularensis* Schu S4 in mice inoculated intradermally (76). These results suggest that the importance of siderophores in virulence may differ depending on the subspecies of *F. tularensis* or the route of infection. Alternatively, FslC may have a function unique from that of FslA that accounts for its greater contribution to virulence. The *feoB*::Tn*5* mutant that we studied was identified as defective for replication in the

lungs of mice after intranasal inoculation in a screen of an LVS transposon library (120). In agreement, we observed that the virulence of both the *feoB*::Tn*5* and the Δ*feoB* mutants was attenuated (Fig. 9B). Neither FslC nor FeoB was essential for causing lethal disease, but both molecules clearly play a part in establishing full virulence of the LVS.

Although complementation of the Δ*fslC* mutation was successful in some circumstances, it failed in others. Production of siderophores by the Δ*fslC* mutant (Fig. 4A and 4B) and its growth in MH II broth with limited ferrous iron (Fig. 5E) were restored by a complementing plasmid. However, the decreased replication of the Δ*fslC* mutant in iron-restricted Che-CDM was not reversed by complementation (Fig. 6B and 6C), and the virulence of the complemented strain in mice was the same as the mutant strain (Fig. 9). These failures might be due to improper regulation of the expression of the gene on the complementing plasmid. Under some circumstances, the growth of the complemented strain was even poorer than that of the uncomplemented Δ*fslC* mutant (Fig. 6B and 6C). Another possible reason is that the *F. tularensis* LVS does not have natural plasmids, and the introduction of a complementing plasmid derived from a *F. novicida* strain might be deleterious. In support of this explanation, we observed that introducing an empty pMP633 plasmid into the Δ*fslC* mutant retarded its growth in iron-restricted media (data not shown). Complementation of the Δ*feoB* mutant was not achieved under any circumstances. Polar effects are unlikely to be the explanation. The *feoB* gene is not in an operon, and the nearest downstream gene is about 800 base pairs away. Furthermore, the deletion in the Δ*feoB* mutant was made in-frame. Notably, the *feoB*::Tn*5* mutant of

the LVS displayed the same behavior as the Δ*feoB* mutant with respect to growth and production of siderophores in media (Fig. 7), replication in hepatocytic cells (Fig. 8), and virulence in mice (Fig. 9). Since two independently derived mutants have a similar phenotype, it is likely that the observed effects are due to inactivation of FeoB.

Our findings raise the possibility that the *F. tularensis* LVS has pathways for acquisition of ferric iron other than siderophores, since the Δ*fslC* mutant grew, albeit slowly, in MH II broth when ferrous iron was chelated (Fig. 5E). A 58-kilodalton protein encoded by FTT0918 in the Schu S4 strain is required for efficient utilization of iron in both siderophore-dependent and -independent manners (76). The LVS, however, does not contain a similar gene, ruling it out as an explanation for our observation. Evidence of another iron acquisition pathway in *F. novicida* was reported by Crosa *et al.* (37). Mutation of the gene FTN_1272, which encodes a putative proton-dependent oligopeptide transporter, results in poorer import of radioactive iron and lower levels of intracellular iron. Genes homologous to FTN_1272 are present in *F. tularensis* Schu S4 (FTT1253) and in the LVS (FTL_0691), but their functions have not been studied. Notably, expression of FTL_0691 was up-regulated 1.5-fold in the LVS growing in hepatocytes (data not shown) and 1.7-fold in the LVS cultured in iron-restricted broth (39). However, we could not delete *fslC* and *feoB* simultaneously despite repeated attempts. This failure suggests that siderophores and FeoB are the major pathways by which the *F. tularensis* LVS takes up iron. If the product of FTL_0691 also contributes to acquisition of iron by the LVS, it is probably very inefficient.

F. tularensis likely requires more than one mechanism to obtain iron due to the many different environments in which it grows. *F. tularensis* has been isolated from water and moist soil. The bacterium also has a broad range of hosts; it infects over 250 animal species, including mammals, birds, fish, invertebrates, and amoebae (44, 116). In mice, viable *F. tularensis* is found both intracellularly and extracellularly in the blood throughout the course of infection (46). We determined here that FslC and FeoB both contribute to the acquisition of iron and virulence in mice, but their functions are not completely redundant. FslC is required for production of siderophores, which provide the bulk of iron when the bacteria grow in niches where ferric iron predominates. FeoB appears more important for replication of the bacterium within cells, at least in the case of hepatocytes. FeoB also contributes to growth of *F. tularensis* before sufficient amounts of siderophores accumulate. Multiple pathways for acquisition of iron thus appear to benefit *F. tularensis* by allowing it to flourish in diverse environments.

II. Response of hepatocytes to infection with *F. tularensis*

The outcomes of infection with *F. tularensis* in vivo depend on multiple spatial and temporal factors, including the routes and times of infection, various hosts, and the subspecies of bacterium used. Dissemination of the bacteria differs depending on the route of inoculation. Intravenous infection leads to enrichment of the bacteria in the liver and spleen within 15 min. Intraperitoneal inoculation also leads to a high bacterial burden in the liver, in this case within 2 h. In contrast, intranasal inoculation results in high levels of bacteria in the lung and gastrointestinal tract, and intradermal inoculation after 20 h

causes only local infection at the site of injection (88). Consequently, host responses to *F. tularensis* are related to the route of infection. For example, intraperitoneal inoculation induces up-regulation of proinflammatory cytokines and chemokines, such as TNF-α, CXCL1, CCL2, IFN-γ, and Nos2, in the liver two days after infection. However, at the same time point, intradermal inoculation causes milder expression of these factors in the liver (29).

The liver is a major target of *F. tularensis*. After intravenous inoculation of the LVS, neutrophils are the first cells marshaled to the liver of mice at 16 h post-infection. The accumulated neutrophils are critical for lysis of the infected hepatocytes and the release and destruction of the intracellular bacteria (31). Blockade of recruitment or depletion of neutrophils leads to extensive replication of the LVS in hepatocytes (31) and a higher number of bacteria in the skin, liver, spleen, and lung (117). However, it is obvious that neutrophils are not sufficient to control the infection in the liver. The percentage of neutrophils in the blood of infected mice increases at early stages of infection, but declines two days later. Mononuclear cells, especially Mac-1^{+} macrophages and myeloid-derived suppressor cells, predominate in the granulomas observed five days after intradermal inoculation (103). However, it is not known how these cells are recruited into the liver at different stages of infection. Resident and/or recruited immune cells, such as macrophages and dendritic cells, may be a source of chemokines and cytokines that attract circulating leukocytes to the area of infection. The LVS induces production of TNF-α, IFN-γ, IL-12 p40, IL-1β, CXCL1, and CCL5 by murine

macrophages through the TLR2 signaling pathway (30). IFN-γ in turn stimulates dendritic cells to produce CXCL9, which can both recruit T cells and optimize interactions among activated T cells, B cells, and dendritic cells to limit infection with *F. tularensis* (92). However, it is also possible that hepatocytes contribute to recruitment of leukocytes in the tularemic liver.

To explore whether hepatocytes have this potential ability, the gene expression profile of murine AML12 hepatocytic cells was assessed by microarray analysis. Indeed, expression of genes encoding a variety of proinflammatory cytokines and chemokines was upregulated, including *Csf3*, *Cxcl2*, *Csf2*, *Ccl20*, *Saa3*, *Cxcl1*, *Tlr2*, *Cxcl5*, *Icam1*, *Csf1*, *Cxcl16*, and *Ccl7* (Table 5). Production of CSF3, CXCL2, and CCL20 was further verified at the protein level (Fig. 10). Colony-stimulating factors, such as CSF1 and CSF3, promote the differentiation and activation of macrophages and neutrophils (54). Chemokines, of which several were up-regulated, are required for the migration of immune cells from the bone marrow to the bloodstream and from the bloodstream to foci of infection. The adhesion molecule ICAM-1 is required for recruitment of leukocytes to hepatic sites of infection (115). These data suggest that hepatocytes might help to attract immune cells to tissues infected with *F. tularensis*.

The genes up-regulated more than 2-fold at 6 h post-infection were analyzed using an online server called the Database for Annotation, Visualization and Integrated Discovery (DAVID; http://david.abcc.ncifcrf.gov/home.jsp). Analysis showed that the up-regulated genes encode cytokines involved in the inflammatory response, chemokines,

cytokine receptors, and components of nuclear factor kappa-light-chain-enhancer of activated B cells (NF-κB), Janus kinase-signal transducer and activator of transcription (JAK-STAT), and mitogen-activated protein kinase (MAPK) signaling pathways. The analysis also demonstrated that the most down-regulated genes encode phosphoproteins and proteins involved in binding, replication, and metabolism of DNA (data not shown). Thus, infection with the LVS induced a global change of gene expression in AML12 hepatocytic cells. This altered expression indicates that hepatocytes *in vivo* may respond to infection with *F. tularensis* by producing proinflammatory cytokines, chemokines, adhesion molecules, and signaling components.

Though expression of *Nos2* was up-regulated in AML12 cells during infection with the LVS, no production of nitric oxide was detected in the conditioned media of infected cells (data not shown). Furthermore, addition of the Nos2 inhibitor L-NMMA did not influence the intracellular growth of bacteria (Fig. 11). Nitric oxide is important for control of replication of *F. tularensis* in the liver of mice, and *Nos2*-deficient mice have a smaller number of hepatic granulomas after infection with the bacterium (14). Taken together, these observations suggest that either hepatocytes are not the source of nitric oxide in tularemic livers or that production of nitric oxide by hepatocytes requires signals in addition to infection.

Notably, the microarray data showed that expression of hepcidin was also up-regulated in infected AML12 hepatocytes. Hepatocytes are the main source of hepcidin in the host (48), and this hormone prevents export of intracellular iron. This

observation suggests that infection with the LVS alters iron metabolism of the host or that the host responds to infection by changing iron distribution through hepcidin.

IFN-γ inhibited the replication of the *F. tularensis* LVS in hepatocytes (Fig. 12). IFN-γ is a key mediator for controlling the progression of tularemia in the liver. NK cells and T cells are the main sources of IFN-γ, and production of IFN-γ requires co-activation signals from IL-12 and IL-18 produced in the liver (134). *In vivo*, IFN-γ regulates the formation of granulomas by restricting the spread of *F. tularensis* LVS within the region of granulomas. Production of Nos2 is absent in IFN-γ-deficient mice but present in the area of granulomas in wild-type mice (14, 134). Although nitric oxide was not produced by IFN-γ treated AML12 cells (data not shown), we do not yet know whether hepatocytes simultaneously treated with IFN-γ and infected with *F. tularensis* make nitric oxide.

III. Significance and future directions

A. Pathways for acquisition of iron

The results of this dissertation project expand the knowledge of iron acquisition pathways of *F. tularensis*, but more remains to be learned. For unknown reasons, the phenotype of the mutant strains was not restored by complementing plasmids in all cases. It is possible that the plasmids themselves are deleterious to the bacterium. It therefore would be worthwhile to complement the mutants by integrating the wild-type genes into the chromosome of the LVS (78). To obtain direct evidence that FslC and FeoB are involved in acquisition of iron, the ability of the mutant strains and the wild-type bacteria to take up radioactive iron could be compared. The dependence of intracellular

replication and virulence on the ability to acquire iron was determined for the *F. tularensis* LVS, but it would be valuable to explore whether FeoB also contributes to virulence of type A strains. It seems that highly virulent type A *F. tularensis* strains possess more options to obtain iron, such as the Fe utilization protein A (FupA) (76), which is absent in the LVS. Deletion of FupA attenuates the virulence of the type A *F. tularensis* Schu S4 strain (128). It is possible that a poorer ability to acquire iron is a factor in the attenuation of the LVS, so it would be of interest to determine whether introduction of *fupA* would increase its virulence in mice. Results of this dissertation work also suggest that besides siderophores and the FeoB pathway, the LVS possesses other mechanisms for uptake of iron with relatively low efficiency. As iron is an essential nutrient for *F. tularensis* and uptake of iron is related to virulence, pathways for acquisition of iron may be a target for development of vaccines. A live vaccine strain genetically manipulated to have limited ability to obtain iron, poor replication in cells, and highly attenuated virulence might be created.

B. Response of hepatocytes to infection with *F. tularensis*

With respect to the host response to *F. tularensis*, this dissertation project provides some clues for the potential role of hepatocytes, which has not been previously explored. Murine hepatocytes control infection with *Listeria monocytogenes* through the NF-κB signaling pathway by recruiting immune cells to foci of infection (72), and it is possible that hepatocytes play a similar part in tularemia. AML12 cells infected with the LVS produced proinflammatory molecules, indicating that hepatocytes may be able to

cooperate with the immune system to combat infection with *F. tularensis*. It is important, though, to study how cultured primary hepatocytes respond to infection, as their behavior may differ from that of hepatocytic cell lines.

However, infection of hepatocytic cell lines or even primary hepatocytes *in vitro* is an artificial model, which might differ in important ways from the case *in vivo*. Hepatic tularemia *in vivo* is far more complicated with various factors involved, including diverse types of cells, cytokines, chemokines, and plasma proteins. It is reasonable to propose that these various factors cooperate as a whole to fight against infection with *F. tularensis*, and it is of interest to understand how hepatocytes participate in this team effort. *In situ* study of hepatocytes in the liver therefore is essential to thoroughly understand their roles in tularemia. For example, *in situ* analysis of the expression of genes of interest in hepatocytes will provide a more complete picture of how they cooperate with the immune system. Conditional knock-down of components of signaling pathways, such as TLR2 or NF-κB, in murine hepatocytes might be informative for understanding their roles in an animal model of tularemia. Additionally, co-cultivation models can be developed to study how hepatocytes communicate with other types of cells in the liver, such as Kupffer cells and NK cells, in the context of tularemia.

As mentioned, IFN-γ is an important cytokine for controlling the progression of tularemia. This work demonstrated that treatment with IFN-γ induced AML12 cells to produce CCL5, which is a chemokine for T cells and also an activator of NK cells (80). It would be of interest to further investigate how IFN-γ regulates the immune response

against tularemia. In addition to our finding that IFN-γ is critical for inhibiting the growth of the *F. tularensis* LVS in hepatocytes, it also inhibits the replication of *F. tularensis* in macrophages (42, 57). The mechanism of this inhibition is not known, and it would be of value to determine whether reactive oxygen or nitrogen species are involved in the process. IFN-γ down-regulates expression of transferrin receptors and lowers the level of iron in human monocytes to inhibit the intracellular growth of *Legionella pneumophila* (21). Consequently, it would be of interest to determine whether IFN-γ influences the content of iron in hepatocytes. Since mutants of the LVS that are defective in production of siderophores and FeoB have been constructed in this work, their ability to replicate in IFN-γ-treated hepatocytes can be assessed.

REFERENCES

1. **Abdul-Tehrani, H., A. J. Hudson, Y. S. Chang, A. R. Timms, C. Hawkins, J. M. Williams, P. M. Harrison, J. R. Guest, and S. C. Andrews**. 1999. Ferritin mutants of *Escherichia coli* are iron deficient and growth impaired, and fur mutants are iron deficient. J. Bacteriol. **181**:1415-1428.

2. **Akira, S., S. Uematsu, and O. Takeuchi**. 2006. Pathogen recognition and innate immunity. Cell **124**:783-801.

3. **Allard, K. A., V. K. Viswanathan, and N. P. Cianciotto**. 2006. lbtA and lbtB are required for production of the *Legionella pneumophila* siderophore legiobactin. J. Bacteriol. **188**:1351-1363.

4. **Anda, P., P. J. Segura del, J. M. Díaz García, R. Escudero, F. J. García Peña, M. C. López Velasco, R. E. Sellek, M. R. Jiménez Chillarón, L. P. Sánchez Serrano, and J. F. Martí nez Navarro**. 2001. Waterborne outbreak of tularemia associated with crayfish fishing. Emerg. Infect. Dis. **7**:575-582.

5. **Andersson, H., B. Hartmanová, R. Kuolee, P. Rydén, W. Conlan, W. Chen, and A. Sjöstedt**. 2006. Transcriptional profiling of host responses in mouse lungs following aerosol infection with type A *Francisella tularensis*. J. Med. Microbiol. **55**:263-271.

6. **Andrews, N. C.** 2000. Iron homeostasis: insights from genetics and animal models. Nat. Rev. Genet. **1**:208-217.

7. **Andrews, S. C., A. K. Robinson, and F. Rodríguez-Quiñones**. 2003. Bacterial iron homeostasis. FEMS Microbiol. Rev. **27**:215-237.

8. **Anthony, L. S., P. J. Morrissey, and F. E. Nano**. 1992. Growth inhibition of *Francisella tularensis* live vaccine strain by IFN-gamma-activated macrophages is mediated by reactive nitrogen intermediates derived from L-arginine metabolism. J. Immunol. **148**:1829-1834.

9. **Bakshi, C. S., M. Malik, M. Mahawar, G. S. Kirimanjeswara, K. R. Hazlett, L. E. Palmer, M. B. Furie, R. Singh, J. A. Melendez, T. J. Sellati, and D. W. Metzger**. 2008. An improved vaccine for prevention of respiratory tularemia caused by *Francisella tularensis* SchuS4 strain. Vaccine **26**:5276-5288.

10. **Barnes, P. J.** 2008. The cytokine network in asthma and chronic obstructive pulmonary disease. J. Clin. Invest **118**:3546-3556.

11. **Baron, G. S. and F. E. Nano**. 1998. MglA and MglB are required for the intramacrophage growth of *Francisella novicida*. Mol. Microbiol. **29**:247-259.

12. **Beinert, H., R. H. Holm, and E. Munck**. 1997. Iron-sulfur clusters: nature's modular, multipurpose structures. Science **277**:653-659.

13. **Berg, R. E., C. J. Cordes, and J. Forman**. 2002. Contribution of CD8+ T cells to innate immunity: IFN-gamma secretion induced by IL-12 and IL-18. Eur. J. Immunol. **32**:2807-2816.

14. **Bokhari, S. M., K. J. Kim, D. M. Pinson, J. Slusser, H. W. Yeh, and M. J. Parmely**. 2008. NK cells and gamma interferon coordinate the formation and function of hepatic granulomas in mice infected with the *Francisella tularensis* live vaccine strain. Infect. Immun. **76**:1379-1389.

15. **Bolger, C. E., C. A. Forestal, J. K. Italo, J. L. Benach, and M. B. Furie**. 2005. The live vaccine strain of *Francisella tularensis* replicates in human and murine macrophages but induces only the human cells to secrete proinflammatory cytokines. J. Leukoc. Biol. **77**:893-897.

16. **Breslow, J. L., H. R. Sloan, V. J. Ferrans, J. L. Anderson, and R. I. Levy**. 1973. Characterization of the mouse liver cell line FL83B. Exp. Cell Res. **78**:441-453.

17. **Brotcke, A., D. S. Weiss, C. C. Kim, P. Chain, S. Malfatti, E. Garcia, and D. M. Monack**. 2006. Identification of MglA-regulated genes reveals novel virulence factors in *F. tularensis*. Infect. Immun. **74**:6642-6655.

18. **Buchan, B. W., R. L. McCaffrey, S. R. Lindemann, L. A. Allen, and B. D. Jones**. 2009. Identification of migR, a regulatory element of the *Francisella tularensis* live vaccine strain *iglABCD* virulence operon required for normal replication and trafficking in macrophages. Infect. Immun. **77**:2517-2529.

19. **Buchan, B. W., M. K. McLendon, and B. D. Jones**. 2008. Identification of differentially regulated *Francisella tularensis* genes by use of a newly developed Tn*5*-based transposon delivery system. Appl. Environ. Microbiol. **74**:2637-2645.

20. **Bullen, J. J., H. J. Rogers, and E. Griffiths**. 1978. Role of iron in bacterial infection. Curr. Top. Microbiol. Immunol. **80**:1-35.

21. **Byrd, T. F. and M. A. Horwitz**. 1989. Interferon gamma-activated human monocytes downregulate transferrin receptors and inhibit the intracellular multiplication of *Legionella pneumophila* by limiting the availability of iron. J. Clin. Invest **83**:1457-1465.

22. **Calvano, S. E., W. Xiao, D. R. Richards, R. M. Felciano, H. V. Baker, R. J. Cho, R. O. Chen, B. H. Brownstein, J. P. Cobb, S. K. Tschoeke, C. Miller-Graziano, L. L. Moldawer, M. N. Mindrinos, R. W. Davis, R. G. Tompkins, and S. F. Lowry**. 2005. A network-based analysis of systemic inflammation in humans. Nature **437**:1032-1037.

23. **Campodonico, V. L., M. Gadjeva, C. Paradis-Bleau, A. Uluer, and G. B. Pier**. 2008. Airway epithelial control of *Pseudomonas aeruginosa* infection in cystic fibrosis. Trends Mol. Med. **14**:120-133.

24. **Cartron, M. L., S. Maddocks, P. Gillingham, C. J. Craven, and S. C. Andrews**. 2006. Feo--transport of ferrous iron into bacteria. Biometals **19**:143-157.

25. **Chamberlain, R. E.** 1965. Evaluation of live tularemia vaccine prepared in a chemically defined medium. Appl. Microbiol. **13**:232-235.

26. **Chen, Y., H. Wei, B. Gao, Z. Hu, S. Zheng, and Z. Tian**. 2005. Activation and function of hepatic NK cells in hepatitis B infection: an underinvestigated innate immune response. J. Viral Hepat. **12**:38-45.

27. **Cherwonogrodzky, J. W., M. H. Knodel, and M. R. Spence**. 1994. Increased encapsulation and virulence of *Francisella tularensis* live vaccine strain (LVS) by subculturing on synthetic medium. Vaccine **12**:773-775.

28. **Clemens, D. L., B. Y. Lee, and M. A. Horwitz**. 2005. *Francisella tularensis* enters macrophages via a novel process involving pseudopod loops. Infect. Immun. **73**:5892-5902.

29. **Cole, L. E., K. L. Elkins, S. M. Michalek, N. Qureshi, L. J. Eaton, P. Rallabhandi, N. Cuesta, and S. N. Vogel**. 2006. Immunologic consequences of *Francisella tularensis* live vaccine strain infection: role of the innate immune response in infection and immunity. J. Immunol. **176**:6888-6899.

30. **Cole, L. E., K. A. Shirey, E. Barry, A. Santiago, P. Rallabhandi, K. L. Elkins, A. C. Puche, S. M. Michalek, and S. N. Vogel**. 2007. Toll-like receptor 2-mediated signaling requirements for *Francisella tularensis* live vaccine strain infection of murine macrophages. Infect. Immun. **75**:4127-4137.

31. **Conlan, J. W. and R. J. North**. 1992. Early pathogenesis of infection in the liver with the facultative intracellular bacteria *Listeria monocytogenes*, *Francisella tularensis*, and *Salmonella typhimurium* involves lysis of infected hepatocytes by leukocytes. Infect. Immun. **60**:5164-5171.

32. **Cornelissen, C. N. and P. F. Sparling**. 1994. Iron piracy: acquisition of transferrin-bound iron by bacterial pathogens. Mol. Microbiol. **14**:843-850.

33. **Cowart, R. E.** 2002. Reduction of iron by extracellular iron reductases: implications for microbial iron acquisition. Arch. Biochem. Biophys. **400**:273-281.

34. **Cowley, S. C. and K. L. Elkins**. 2003. Multiple T cell subsets control *Francisella tularensis* LVS intracellular growth without stimulation through macrophage interferon gamma receptors. J. Exp. Med. **198**:379-389.

35. **Crispe, I. N.** 2009. The liver as a lymphoid organ. Annu. Rev. Immunol. **27**:147-163.

36. **Cronquist, S. D.** 2004. Tularemia: the disease and the weapon. Dermatol. Clin. **22**:313-320.

37. **Crosa, L. M., J. H. Crosa, and F. Heffron**. 2009. Iron transport in *Francisella* in the absence of a recognizable TonB protein still requires energy generated by the proton motive force. Biometals **22**:337-344.

38. **Dame, T. M., B. L. Orenzoff, L. E. Palmer, and M. B. Furie**. 2007. IFN-gamma alters the response of *Borrelia burgdorferi*-activated endothelium to favor chronic inflammation. J. Immunol. **178**:1172-1179.

39. **Deng, K., R. J. Blick, W. Liu, and E. J. Hansen**. 2006. Identification of *Francisella tularensis* genes affected by iron limitation. Infect. Immun. **74**:4224-4236.

40. **Dennis, D. T., T. V. Inglesby, D. A. Henderson, J. G. Bartlett, M. S. Ascher, E. Eitzen, A. D. Fine, A. M. Friedlander, J. Hauer, M. Layton, S. R. Lillibridge, J. E. McDade, M. T. Osterholm, T. O'Toole, G. Parker, T. M. Perl, P. K. Russell, and K. Tonat**. 2001. Tularemia as a biological weapon: medical and public health management. JAMA **285**:2763-2773.

41. **Doherty, C. P.** 2007. Host-pathogen interactions: the role of iron. J. Nutr. **137**:1341-1344.

42. **Edwards, J. A., D. Rockx-Brouwer, V. Nair, and J. Celli**. 2010. Restricted cytosolic growth of *Francisella tularensis* subsp. tularensis by IFN-gamma activation of macrophages. Microbiology **156**:327-339.

43. **Ellis, J., P. C. Oyston, M. Green, and R. W. Titball**. 2002. Tularemia. Clin. Microbiol. Rev. **15**:631-646.

44. **Foley, J. E. and N. C. Nieto**. 2010. Tularemia. Vet. Microbiol. **140**:332-338.

45. **Forestal, C. A., J. L. Benach, C. Carbonara, J. K. Italo, T. J. Lisinski, and M. B. Furie**. 2003. *Francisella tularensis* selectively induces proinflammatory changes in endothelial cells. J. Immunol. **171**:2563-2570.

46. **Forestal, C. A., M. Malik, S. V. Catlett, A. G. Savitt, J. L. Benach, T. J. Sellati, and M. B. Furie**. 2007. *Francisella tularensis* has a significant extracellular phase in infected mice. J. Infect. Dis. **196**:134-137.

47. **Fortier, A. H., M. V. Slayter, R. Ziemba, M. S. Meltzer, and C. A. Nacy**. 1991. Live vaccine strain of *Francisella tularensis*: infection and immunity in mice. Infect. Immun. **59**:2922-2928.

48. **Franchini, M., M. Montagnana, and G. Lippi**. 2010. Hepcidin and iron metabolism: from laboratory to clinical implications. Clin. Chim. Acta. doi:doi:10.1016/j.cca.2010.07.003.

49. **Gao, B., W. I. Jeong, and Z. Tian**. 2008. Liver: An organ with predominant innate immunity. Hepatology **47**:729-736.

50. **Gentleman, R. C., V. J. Carey, D. M. Bates, B. Bolstad, M. Dettling, S. Dudoit, B. Ellis, L. Gautier, Y. Ge, J. Gentry, K. Hornik, T. Hothorn, W. Huber, S. Iacus, R. Irizarry, F. Leisch, C. Li, M. Maechler, A. J. Rossini, G. Sawitzki, C. Smith, G. Smyth, L. Tierney, J. Y. Yang, and J. Zhang**. 2004. Bioconductor: open software development for computational biology and bioinformatics. Genome Biol. **5**:R80.

51. **Golovliov, I., K. Kuoppa, A. Sjöstedt, A. Tärnvik, and G. Sandström**. 1996. Cytokine expression in the liver of mice infected with a highly virulent strain of *Francisella tularensis*. FEMS Immunol. Med. Microbiol. **13**:239-244.

52. **Golovliov, I., G. Sandström, M. Ericsson, A. Sjöstedt, and A. Tärnvik**. 1995. Cytokine expression in the liver during the early phase of murine tularemia. Infect. Immun. **63**:534-538.

53. **Gregory, S. H. and E. J. Wing**. 1993. IFN-gamma inhibits the replication of *Listeria monocytogenes* in hepatocytes. J. Immunol. **151**:1401-1409.

54. **Hamilton, J. A.** 2008. Colony-stimulating factors in inflammation and autoimmunity. Nat. Rev. Immunol. **8**:533-544.

55. **Hantke, K.** 2003. Is the bacterial ferrous iron transporter FeoB a living fossil? Trends Microbiol. **11**:192-195.

56. **Haponsaph, R. and C. J. Czuprynski**. 1996. Inhibition of the multiplication of *Listeria monocytogenes* in a murine hepatocyte cell line (ATCC TIB73) by IFN-gamma and TNF-alpha. Microb. Pathog. **20**:287-295.

57. **Holická, M., J. Novosad, M. Loudová, M. Kudlová, and J. Krejsek**. 2009. The effect of interferon-gamma and lipopolysaccharide on the growth of *Francisella tularensis* LVS in murine macrophage-like cell line J774. Acta Medica. (Hradec. Kralove) **52**:101-106.

58. **Hong, K. J., J. R. Wickstrum, H. W. Yeh, and M. J. Parmely**. 2007. Toll-like receptor 2 controls the gamma interferon response to *Francisella tularensis* by mouse liver lymphocytes. Infect. Immun. **75**:5338-5345.

59. **Hung, K. W., Y. W. Chang, E. T. Eng, J. H. Chen, Y. C. Chen, Y. J. Sun, C. D. Hsiao, G. Dong, K. A. Spasov, V. M. Unger, and T. H. Huang**. 2010. Structural fold, conservation and Fe(II) binding of the intracellular domain of prokaryote FeoB. J. Struct. Biol. **170**:501-512.

60. **Huntley, J. F., P. G. Conley, K. E. Hagman, and M. V. Norgard**. 2007. Characterization of *Francisella tularensis* outer membrane proteins. J. Bacteriol. **189**:561-574.

61. **Janeway, C. A., Jr. and R. Medzhitov**. 2002. Innate immune recognition. Annu. Rev. Immunol. **20**:197-216.

62. **Jin, Y., M. Hattori, H. Nisimasu, R. Ishitani, and O. Nureki**. 2009. Crystallization and preliminary X-ray diffraction analysis of the truncated cytosolic domain of the iron transporter FeoB. Acta Crystallogr. Sect. F. Struct. Biol. Cryst. Commun. **65**:784-787.

63. **Kammler, M., C. Schön, and K. Hantke**. 1993. Characterization of the ferrous iron uptake system of *Escherichia coli*. J. Bacteriol. **175**:6212-6219.

64. **Kawai, T. and S. Akira**. 2006. TLR signaling. Cell Death. Differ. **13**:816-825.

65. **Kiss, K., W. Liu, J. F. Huntley, M. V. Norgard, and E. J. Hansen**. 2008. Characterization of fig operon mutants of *Francisella novicida* U112. FEMS Microbiol. Lett. **285**:270-277.

66. **Koziolek, M. J., R. Vasko, C. Bramlage, G. A. Müller, and F. Strutz**. 2009. The CX(3)C-chemokine fractalkine in kidney diseases. Mini. Rev. Med. Chem. **9**:1215-1228.

67. **Kumagai, Y. and S. Akira**. 2010. Identification and functions of

pattern-recognition receptors. J. Allergy Clin. Immunol. **125**:985-992.

68. **Lai, X. H., I. Golovliov, and A. Sjöstedt**. 2004. Expression of IglC is necessary for intracellular growth and induction of apoptosis in murine macrophages by *Francisella tularensis*. Microb. Pathog. **37**:225-230.

69. **Larson, J. A., H. L. Howie, and M. So**. 2004. *Neisseria meningitidis* accelerates ferritin degradation in host epithelial cells to yield an essential iron source. Mol. Microbiol. **53**:807-820.

70. **Lasta, M., K. Polak, A. Luksch, G. Garhofer, and L. Schmetterer**. 2010. Effect of NO synthase inhibition on retinal vessel reaction to isometric exercise in healthy humans. Acta Ophthalmol. doi:AOS1970 [pii];10.1111/j.1755-3768.2010.01970.x [doi].

71. **Lauriano, C. M., J. R. Barker, S. S. Yoon, F. E. Nano, B. P. Arulanandam, D. J. Hassett, and K. E. Klose**. 2004. MglA regulates transcription of virulence factors necessary for *Francisella tularensis* intraamoebae and intramacrophage survival. Proc. Natl. Acad. Sci. U. S. A **101**:4246-4249.

72. **Lavon, I., I. Goldberg, S. Amit, L. Landsman, S. Jung, B. Z. Tsuberi, I. Barshack, J. Kopolovic, E. Galun, H. Bujard, and Y. Ben-Neriah**. 2000. High susceptibility to bacterial infection, but no liver dysfunction, in mice compromised for hepatocyte NF-kappaB activation. Nat. Med. **6**:573-577.

73. **Lazennec, G. and A. Richmond**. 2010. Chemokines and chemokine receptors: new insights into cancer-related inflammation. Trends Mol. Med. **16**:133-144.

74. **Lenco, J., M. Hubálek, P. Larsson, A. Fucíková, M. Brychta, A. Macela, and J. Stulík**. 2007. Proteomics analysis of the *Francisella tularensis* LVS response to iron restriction: induction of the *F. tularensis* pathogenicity island proteins IglABC. FEMS Microbiol. Lett. **269**:11-21.

75. **Li, X. and S. C. Ricke**. 2003. Generation of an *Escherichia coli* lysA targeted deletion mutant by double cross-over recombination for potential use in a bacterial growth-based lysine assay. Lett. Appl. Microbiol. **37**:458-462.

76. **Lindgren, H., M. Honn, I. Golovlev, K. Kadzhaev, W. Conlan, and A. Sjöstedt**. 2009. The 58-kilodalton major virulence factor of *Francisella tularensis* is required for efficient utilization of iron. Infect. Immun. **77**:4429-4436.

77. **Litwin, C. M. and S. B. Calderwood**. 1993. Role of iron in regulation of virulence genes. Clin. Microbiol. Rev. **6**:137-149.

78. **LoVullo, E. D., C. R. Molins-Schneekloth, H. P. Schweizer, and M. S. Pavelka, Jr.** 2009. Single-copy chromosomal integration systems for Francisella tularensis. Microbiology **155**:1152-1163.

79. **LoVullo, E. D., L. A. Sherrill, L. L. Perez, and M. S. Pavelka, Jr.** 2006. Genetic tools for highly pathogenic *Francisella tularensis* subsp. *tularensis*. Microbiology **152**:3425-3435.

80. **Maghazachi, A. A., A. Al-Aoukaty, and T. J. Schall**. 1996. CC chemokines induce the generation of killer cells from CD56+ cells. Eur. J. Immunol. **26**:315-319.

81. **Maier, T. M., A. Havig, M. Casey, F. E. Nano, D. W. Frank, and T. C. Zahrt**. 2004. Construction and characterization of a highly efficient *Francisella* shuttle plasmid. Appl. Environ. Microbiol. **70**:7511-7519.

82. **McLendon, M. K., M. A. Apicella, and L. A. Allen**. 2006. *Francisella tularensis*: taxonomy, genetics, and immunopathogenesis of a potential agent of biowarfare. Annu. Rev. Microbiol. **60**:167-185.

83. **Meylan, E., J. Tschopp, and M. Karin**. 2006. Intracellular pattern recognition receptors in the host response. Nature **442**:39-44.

84. **Murdoch, C. and A. Finn**. 2000. Chemokine receptors and their role in inflammation and infectious diseases. Blood **95**:3032-3043.

85. **Naikare, H., K. Palyada, R. Panciera, D. Marlow, and A. Stintzi**. 2006. Major role for FeoB in *Campylobacter jejuni* ferrous iron acquisition, gut colonization, and intracellular survival. Infect. Immun. **74**:5433-5444.

86. **Nano, F. E., N. Zhang, S. C. Cowley, K. E. Klose, K. K. Cheung, M. J. Roberts, J. S. Ludu, G. W. Letendre, A. I. Meierovics, G. Stephens, and K. L. Elkins**. 2004. A *Francisella tularensis* pathogenicity island required for intramacrophage growth. J. Bacteriol. **186**:6430-6436.

87. **Noah, C. E., M. Malik, D. C. Bublitz, D. Camenares, T. J. Sellati, J. L. Benach, and M. B. Furie**. 2010. GroEL and lipopolysaccharide from *Francisella tularensis* live vaccine strain synergistically activate human macrophages. Infect. Immun. **78**:1797-1806.

88. **Ojeda, S. S., Z. J. Wang, C. A. Mares, T. A. Chang, Q. Li, E. G. Morris, P. A. Jerabek, and J. M. Teale**. 2008. Rapid dissemination of *Francisella tularensis* and the effect of route of infection. BMC. Microbiol. **8**:215.

89. **Olakanmi, O., L. S. Schlesinger, A. Ahmed, and B. E. Britigan**. 2002.

Intraphagosomal *Mycobacterium tuberculosis* acquires iron from both extracellular transferrin and intracellular iron pools. Impact of interferon-gamma and hemochromatosis. J. Biol. Chem. **277**:49727-49734.

90. **Otto, B. R., M. Sparrius, A. M. Verweij-van Vught, and D. M. MacLaren**. 1990. Iron-regulated outer membrane protein of *Bacteroides fragilis* involved in heme uptake. Infect. Immun. **58**:3954-3958.

91. **Pan, X., B. Tamilselvam, E. J. Hansen, and S. Daefler**. 2010. Modulation of iron homeostasis in macrophages by bacterial intracellular pathogens. BMC. Microbiol. **10**:64.

92. **Park, M. K., D. Amichay, P. Love, E. Wick, F. Liao, A. Grinberg, R. L. Rabin, H. H. Zhang, S. Gebeyehu, T. M. Wright, A. Iwasaki, Y. Weng, J. A. DeMartino, K. L. Elkins, and J. M. Farber**. 2002. The CXC chemokine murine monokine induced by IFN-gamma (CXC chemokine ligand 9) is made by APCs, targets lymphocytes including activated B cells, and supports antibody responses to a bacterial pathogen in vivo. J. Immunol. **169**:1433-1443.

93. **Perry, R. D., I. Mier, Jr., and J. D. Fetherston**. 2007. Roles of the Yfe and Feo transporters of *Yersinia pestis* in iron uptake and intracellular growth. Biometals **20**:699-703.

94. **Petermann, N., G. Hansen, C. L. Schmidt, and R. Hilgenfeld**. 2010. Structure of the GTPase and GDI domains of FeoB, the ferrous iron transporter of *Legionella pneumophila*. FEBS Lett. **584**:733-738.

95. **Petrat, F., G. H. de, and U. Rauen**. 2000. Determination of the chelatable iron pool of single intact cells by laser scanning microscopy. Arch. Biochem. Biophys. **376**:74-81.

96. **Petrat, F., G. H. de, and U. Rauen**. 2001. Subcellular distribution of chelatable iron: a laser scanning microscopic study in isolated hepatocytes and liver endothelial cells. Biochem. J. **356**:61-69.

97. **Pfaffl, M. W.** 2001. A new mathematical model for relative quantification in real-time RT-PCR. Nucleic Acids Res. **29**:e45.

98. **Polsinelli, T., M. S. Meltzer, and A. H. Fortier**. 1994. Nitric oxide-independent killing of *Francisella tularensis* by IFN-gamma-stimulated murine alveolar macrophages. J. Immunol. **153**:1238-1245.

99. **Pope, C. D., W. O'Connell, and N. P. Cianciotto**. 1996. *Legionella pneumophila*

mutants that are defective for iron acquisition and assimilation and intracellular infection. Infect. Immun. **64**:629-636.

100. **Qin, A. and B. J. Mann**. 2006. Identification of transposon insertion mutants of *Francisella tularensis* tularensis strain Schu S4 deficient in intracellular replication in the hepatic cell line HepG2. BMC. Microbiol. **6**:69.

101. **Ramakrishnan, G., A. Meeker, and B. Dragulev**. 2008. fslE is necessary for siderophore-mediated iron acquisition in *Francisella tularensis* Schu S4. J. Bacteriol. **190**:5353-5361.

102. **Ransohoff, R. M.** 2009. Chemokines and chemokine receptors: standing at the crossroads of immunobiology and neurobiology. Immunity. **31**:711-721.

103. **Rasmussen, J. W., J. Cello, H. Gil, C. A. Forestal, M. B. Furie, D. G. Thanassi, and J. L. Benach**. 2006. Mac-1+ cells are the predominant subset in the early hepatic lesions of mice infected with *Francisella tularensis*. Infect. Immun. **74**:6590-6598.

104. **Robey, M. and N. P. Cianciotto**. 2002. *Legionella pneumophila* feoAB promotes ferrous iron uptake and intracellular infection. Infect. Immun. **70**:5659-5669.

105. **Rodriguez, S. A., J. J. Yu, G. Davis, B. P. Arulanandam, and K. E. Klose**. 2008. Targeted inactivation of *Francisella tularensis* genes by group II introns. Appl. Environ. Microbiol. **74**:2619-2626.

106. **Rotz, L. D., A. S. Khan, S. R. Lillibridge, S. M. Ostroff, and J. M. Hughes**. 2002. Public health assessment of potential biological terrorism agents. Emerg. Infect. Dis. **8**:225-230.

107. **Rowell, D. L., L. Eckmann, M. B. Dwinell, S. P. Carpenter, J. L. Raucy, S. K. Yang, and M. F. Kagnoff**. 1997. Human hepatocytes express an array of proinflammatory cytokines after agonist stimulation or bacterial invasion. Am. J. Physiol **273**:G322-G332.

108. **Santic, M., R. Asare, I. Skrobonja, S. Jones, and K. Y. Abu**. 2008. Acquisition of the vATPase proton pump and phagosome acidification is essential for escape of *Francisella tularensis* into the macrophage cytosol. Infect. Immun. **76**:2671-2677.

109. **Santic, M., M. Molmeret, K. E. Klose, and K. Y. Abu**. 2006. *Francisella tularensis* travels a novel, twisted road within macrophages. Trends Microbiol. **14**:37-44.

110. **Santic, M., M. Molmeret, K. E. Klose, S. Jones, and Y. A. Kwaik**. 2005. The

Francisella tularensis pathogenicity island protein IglC and its regulator MglA are essential for modulating phagosome biogenesis and subsequent bacterial escape into the cytoplasm. Cell Microbiol. **7**:969-979.

111. **Saslaw, S., H. T. Eigelsbach, J. A. Prior, H. E. Wilson, and S. Carhart**. 1961. Tularemia vaccine study. II. Respiratory challenge. Arch. Intern. Med. **107**:702-714.

112. **Schaible, U. E., H. L. Collins, and S. H. Kaufmann**. 1999. Confrontation between intracellular bacteria and the immune system. Adv. Immunol. **71**:267-377.

113. **Schaible, U. E. and S. H. Kaufmann**. 2004. Iron and microbial infection. Nat. Rev. Microbiol. **2**:946-953.

114. **Schwyn, B. and J. B. Neilands**. 1987. Universal chemical assay for the detection and determination of siderophores. Anal. Biochem. **160**:47-56.

115. **Shi, C., P. Velazquez, T. M. Hohl, I. Leiner, M. L. Dustin, and E. G. Pamer**. 2010. Monocyte trafficking to hepatic sites of bacterial infection is chemokine independent and directed by focal intercellular adhesion molecule-1 expression. J. Immunol. **184**:6266-6274.

116. **Sjöstedt, A.** 2007. Tularemia: history, epidemiology, pathogen physiology, and clinical manifestations. Ann. N. Y. Acad. Sci. **1105**:1-29.

117. **Sjöstedt, A., J. W. Conlan, and R. J. North**. 1994. Neutrophils are critical for host defense against primary infection with the facultative intracellular bacterium *Francisella tularensis* in mice and participate in defense against reinfection. Infect. Immun. **62**:2779-2783.

118. **Smyth, G. K.** 2004. Linear models and empirical bayes methods for assessing differential expression in microarray experiments. Stat. Appl. Genet. Mol. Biol. **3**:Article3.

119. **Stojiljkovic, I., M. Cobeljic, and K. Hantke**. 1993. *Escherichia coli* K-12 ferrous iron uptake mutants are impaired in their ability to colonize the mouse intestine. FEMS Microbiol. Lett. **108**:111-115.

120. **Su, J., J. Yang, D. Zhao, T. H. Kawula, J. A. Banas, and J. R. Zhang**. 2007. Genome-wide identification of *Francisella tularensis* virulence determinants. Infect. Immun. **75**:3089-3101.

121. **Subleski, J. J., V. L. Hall, T. C. Back, J. R. Ortaldo, and R. H. Wiltrout**. 2006. Enhanced antitumor response by divergent modulation of natural killer and natural killer T cells in the liver. Cancer Res. **66**:11005-11012.

122. **Sullivan, J. T., E. F. Jeffery, J. D. Shannon, and G. Ramakrishnan**. 2006. Characterization of the siderophore of *Francisella tularensis* and role of fslA in siderophore production. J. Bacteriol. **188**:3785-3795.

123. **Szalay, G., J. Hess, and S. H. Kaufmann**. 1995. Restricted replication of *Listeria monocytogenes* in a gamma interferon-activated murine hepatocyte line. Infect. Immun. **63**:3187-3195.

124. **Tarnvik, A. and L. Berglund**. 2003. Tularaemia. Eur. Respir. J. **21**:361-373.

125. **Touati, D.** 2000. Iron and oxidative stress in bacteria. Arch. Biochem. Biophys. **373**:1-6.

126. **Tresselt, H. B. and M. K. Ward**. 1964. Blood-free medium for the rapid growth of *Pasteurella tularensis*. Appl. Microbiol. **12**:504-507.

127. **Tsolis, R. M., A. J. Baumler, F. Heffron, and I. Stojiljkovic**. 1996. Contribution of TonB- and Feo-mediated iron uptake to growth of *Salmonella typhimurium* in the mouse. Infect. Immun. **64**:4549-4556.

128. **Twine, S., M. Bystrom, W. Chen, M. Forsman, I. Golovliov, A. Johansson, J. Kelly, H. Lindgren, K. Svensson, C. Zingmark, W. Conlan, and A. Sjostedt**. 2005. A mutant of *Francisella tularensis* strain SCHU S4 lacking the ability to express a 58-kilodalton protein is attenuated for virulence and is an effective live vaccine. Infect. Immun. **73**:8345-8352.

129. **Van Amersfoort, E. S., T. J. Van Berkel, and J. Kuiper**. 2003. Receptors, mediators, and mechanisms involved in bacterial sepsis and septic shock. Clin. Microbiol. Rev. **16**:379-414.

130. **Velayudhan, J., N. J. Hughes, A. A. McColm, J. Bagshaw, C. L. Clayton, S. C. Andrews, and D. J. Kelly**. 2000. Iron acquisition and virulence in *Helicobacter pylori*: a major role for FeoB, a high-affinity ferrous iron transporter. Mol. Microbiol. **37**:274-286.

131. **Viswanathan, V. K., P. H. Edelstein, C. D. Pope, and N. P. Cianciotto**. 2000. The *Legionella pneumophila* iraAB locus is required for iron assimilation, intracellular infection, and virulence. Infect. Immun. **68**:1069-1079.

132. **Wehrly, T. D., A. Chong, K. Virtaneva, D. E. Sturdevant, R. Child, J. A. Edwards, D. Brouwer, V. Nair, E. R. Fischer, L. Wicke, A. J. Curda, J. J. Kupko, III, C. Martens, D. D. Crane, C. M. Bosio, S. F. Porcella, and J. Celli**. 2009. Intracellular biology and virulence determinants of *Francisella tularensis*

revealed by transcriptional profiling inside macrophages. Cell Microbiol. **11**:1128-1150.

133. **Wickstrum, J. R., S. M. Bokhari, J. L. Fischer, D. M. Pinson, H. W. Yeh, R. T. Horvat, and M. J. Parmely**. 2009. *Francisella tularensis* induces extensive caspase-3 activation and apoptotic cell death in the tissues of infected mice. Infect. Immun. **77**:4827-4836.

134. **Wickstrum, J. R., K. J. Hong, S. Bokhari, N. Reed, N. McWilliams, R. T. Horvat, and M. J. Parmely**. 2006. Co-activating signals for the hepatic lymphocyte interferon-γ response to *Francisella tularensis*. Infect. Immun. **75**:1335-1342.

135. **Williams, P. H. and P. J. Warner**. 1980. ColV plasmid-mediated, colicin V-independent iron uptake system of invasive strains of *Escherichia coli*. Infect. Immun. **29**:411-416.

136. **Worst, D. J., M. M. Gerrits, C. M. Vandenbroucke-Grauls, and J. G. Kusters**. 1998. Helicobacter pylori ribBA-mediated riboflavin production is involved in iron acquisition. J. Bacteriol. **180**:1473-1479.

137. **Wu, J. C., G. Merlino, and N. Fausto**. 1994. Establishment and characterization of differentiated, nontransformed hepatocyte cell lines derived from mice transgenic for transforming growth factor alpha. Proc. Natl. Acad. Sci. U. S. A **91**:674-678.

138. **Yan, W., H. Lee, E. W. Deutsch, C. A. Lazaro, W. Tang, E. Chen, N. Fausto, M. G. Katze, and R. Aebersold**. 2004. A dataset of human liver proteins identified by protein profiling via isotope-coded affinity tag (ICAT) and tandem mass spectrometry. Mol. Cell Proteomics. **3**:1039-1041.